Carnets Geol. 23 (7)

E-ISSN 1634-0744
DOI 10.2110/carnets.2023.2307

Hiatuses and redeposits in the Tithonian-Berriasian transition at Le Chouet (Les Près, La Drôme, SE France): Sedimentological and biostratigraphical implications

Bruno R.C. GRANIER [1]
Serge FERRY [2]
Mohamed BENZAGGAGH [3]

Abstract: Our new study of the Tithonian and lower Berriasian succession of Le Chouet (Les Près, La Drôme, France) better characterizes the lithological succession, the macro- and microfacies, and the stratigraphic ranges of some microfossils mostly calibrated on the calpionellid biozonation. On the lithological side, the Tithonian strata are dominantly characterized by thick-bedded breccias representing debris flows and related calciturbidites whereas the Berriasian strata are typically white limestones that also comprises scattered intercalations of thin-bedded breccias and calciturbitides (including cryptic mud calciturbidites). In thin sections, these white limestones display mud- to wackestone textures and their allochems are mostly tiny bioclasts (*e.g.*, radiolarians, calpionellids, saccocomids). Breccias are lithoclastic rudstones and/or floatstones with a matrix similar to the calciturbidites. Their lithoclasts are either extraclasts *sensu stricto* (*i.e.*, material derived from updip shallow-water areas) or pseudointraclasts, representing reworked subautochthonous material (*i.e.*, mud- and wackestone lithoclasts with radiolarians, saccocomids and/or calpionellids). In addition to the erosional features observed at the bases of the gravity flows, these pseudointraclasts document the intensity of submarine erosion. Locally they help to estimate the depths of erosion updip of the deposit. A number of bioclasts are reworked from updip shallow-water areas; among them, it is worth mentioning the foraminifer *Protopeneroplis ultragranulata* (GORBATCHIK), the first occurrence of which is dated to late early Tithonian. Saccocomids are part of the dominating pelagic biota reported from the lower and lower upper Tithonian interval whereas calpionellids replace them in the uppermost Tithonian to lower Berriasian interval. Intervals with saccocomids characteristic of zones 4-5 and zones 6-7 are respectively ascribed here to the lower Tithonian (4-5) and *pro parte* to the upper Tithonian (6-7). The biozonation of the calpionellid group *sensu lato* allows identification of the Boneti Subzone of the chitinoidellids, the Crassicollaria Zone with its four subzones (A0-A3), and the Alpina Zone with its first subzone (B1). On the basis of biostratigraphical and sedimentological data (including the rates of sedimentation), most zonal boundaries are located at the erosional bases of breccia or turbidite layers and thus coincide with hiatuses.

Keywords:

- Tithonian;
- Berriasian;
- calpionellids;
- saccocomids;
- erosion;
- debris flows;
- turbidites;
- lithoclasts;
- Vocontian Trough

Citation: GRANIER B.R.C., FERRY S. & BENZAGGAGH M. (2023).- Hiatuses and redeposits in the Tithonian-Berriasian transition at Le Chouet (Les Près, La Drôme, SE France): Sedimentological and biostratigraphical implications.- *Carnets Geol.*, Madrid, vol. 23, no. 7, p. 123-147.

[1] *Dépt. STU, Fac. Sci. Tech., UBO, 6 avenue Le Gorgeu, CS 93837, F-29238 Brest (France)*
bgranier@univ-brest.fr

[2] *6D avenue Général de Gaulle, F-05200 Briançon (France)*
serge.ferry@yahoo.fr

[3] *Department of Geology, Moulay Ismail University, Meknes (Morocco)*
benzaggagh@gmail.com

Published online in final form (pdf) on June 27, 2023
[Editor: Michel MOULLADE; language editor: Phil SALVADOR; technical editor: Bruno GRANIER]

Résumé : ***Lacunes et redéposition à la transition Tithonien-Berriasien au Chouet (Les Près, Drôme, SE France) : Implications sédimentologiques et biostratigraphiques.-*** Notre nouvelle étude de la succession du Tithonien au Berriasien inférieur du Chouet (Les Près, Drôme, France) précise la succession lithologique, les macro- et microfaciès, et les répartitions stratigraphiques de quelques microfossiles essentiellement calibrées ici sur la biozonation des calpionellidés. D'un point de vue lithologique, les dépôts du Tithonien sont principalement représentés par des brèches en bancs épais représentant des coulées de débris et par des calciturbidites associées, tandis que les dépôts du Berriasien sont typiquement constitués de calcaires blancs qui recèlent également des intercalations éparses de passées bréchiques et de calciturbitides (y compris des calciturbidites de boue, souvent cryptiques). En lames minces, ces calcaires blancs présentent des textures mud- à wackestone et leurs éléments figurés sont pour la plupart de minuscules bioclastes (comme, par exemple, des radiolaires, des calpionellidés, des saccocomidés). Les brèches sont des rud- et/ou floatstones lithoclastiques avec une matrice comparable aux calciturbidites. Leurs lithoclastes sont soit des extraclastes *sensu stricto* (c'est-à-dire du matériel remanié de zones peu profondes en amont), soit des pseudo-intraclastes, représentant du matériel sub-autochtone remanié (c'est-à-dire des lithoclastes à textures mud- à wackestone avec des radiolaires, des saccocomidés et/ou des calpionellidés). Outre les structures liées à l'érosion observées à la base des écoulements gravitaires, ces pseudo-intraclastes témoignent de l'intensité de l'érosion sous-marine. Localement, ils permettent d'estimer les profondeurs d'érosion en amont des coulées. Un nombre non négligeable de bioclastes sont remaniés de zones peu profondes en amont, parmi lesquels il convient de mentionner le foraminifère *Protopeneroplis ultragranulata* (Gorbatchik), dont la première apparition est datée ici du Tithonien inférieur terminal. Les saccocomidés font partie des organismes pélagiques dominants signalés dans l'intervalle Tithonien inférieur à supérieur, tandis que les calpionelles les remplacent dans l'intervalle Tithonien supérieur à Berriasien inférieur. Les intervalles à saccocomidés, caractéristiques des zones 4-5 ainsi que des zones 6-7, sont respectivement attribués ici au Tithonien inférieur (4-5) ainsi que *pro parte* au Tithonien supérieur (6-7). La biozonation du groupe des calpionelles *sensu lato* permet l'identification de la Sous-Zone à Boneti des chitinoïdellidés, la Zone à Crassicollaria avec ses quatre sous-zones (A0-A3) et la Zone à Alpina avec sa première sous-zone (B1). Sur la base de données sédimentologiques (y compris les taux de sédimentation) et biostratigraphiques, la plupart des limites de zones sont localisées aux bases érosives de couches de brèches ou de turbidites et correspondent donc à des lacunes sédimentaires.

Mots-clefs :

- Tithonien ;
- Berriasien ;
- calpionellidés ;
- saccocomidés ;
- érosion ;
- coulées de débris ;
- turbidites ;
- lithoclastes ;
- Fosse vocontienne

1. Introduction

In parallel with recent investigations on the former Berriasian GSSP candidate at Tré Maroua, Le Saix, Hautes-Alpes (Granier *et al.*, 2020b, 2022, 2023), our group studied another key section of the Vocontian Trough (SE France) for the Tithonian-Berriasian transition at Le Chouet, Les Près, La Drôme (Ferry & Granier, 2018). This second section (Figs. 1-2) was studied by Remane (1970: Fig. 6) and by the former Berriasian Working Group (Wimbledon *et al.*, 2013: Fig. 4, 2020a: Supplement Fig. S1). Its ammonite fauna was first studied by Le Hégarat (1973) but it did not prove to be useful because the author's log (*op.cit.*: Fig. 25) cannot be correlated with any of the other logs. The Le Chouet section partly spans two lithostratigraphic units: 1) the uppermost part of the "brèches tithoniennes" (Tithonian breccias) below and 2) the lower part of the "calcaires blancs vocontiens" (Vocontian white limestones) above. However, as shown in the logs (Figs. 2-3), facies separation is no so clear cut: lime mudstone layers sporadically occur between conglomeratic beds of the Tithonian breccias whereas conglomeratic layers locally occur in the white limestones. This pattern merely reflects the decreasing intensity of the resedimentation over the Tithonian-Berriasian transition. Only the dominant type of macrofacies justifies this subdivision.

Contrary to Remane (1970), Wimbledon *et al.* (2013, 2020a) have mostly neglected the sedimentological aspects of the Le Chouet section. More specifically they underestimated the gravity-flow erosion and the redeposition of the derived material that obviously impacted the apparent continuity of the sedimentary record. As will be demonstrated below, although that is not always visible at the scale of temporal resolution of the ammonite zones or that of the calpionellids, the logged section is hiatal. It was already the case for the former Berriasian GSSP candidate at Tré Maroua, Le Saix, Hautes-Alpes (Granier *et al.*, 2020b, 2022, 2023).

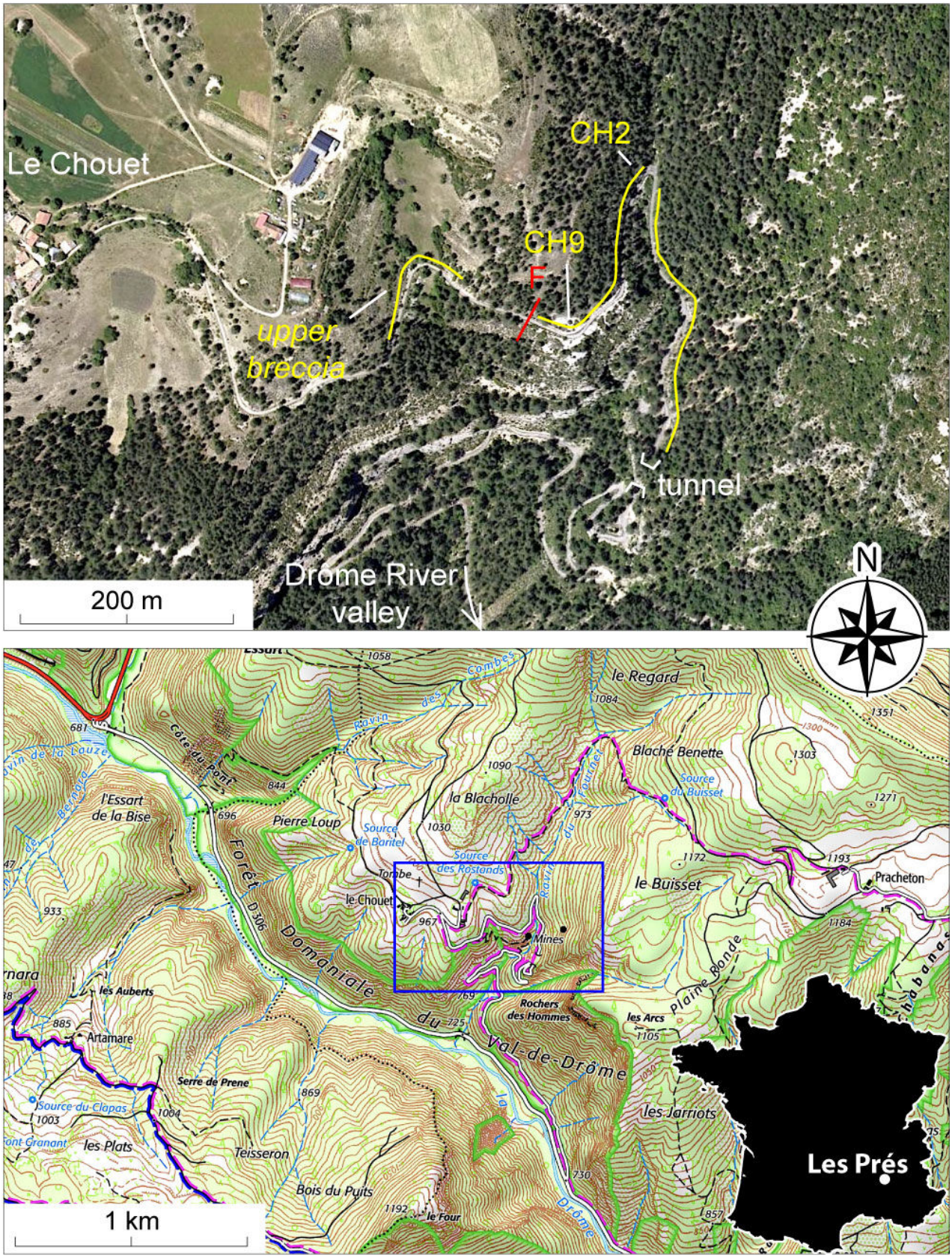

Figure 1: Topographic map of the Le Chouet area (A) and location of the sections studied (B).

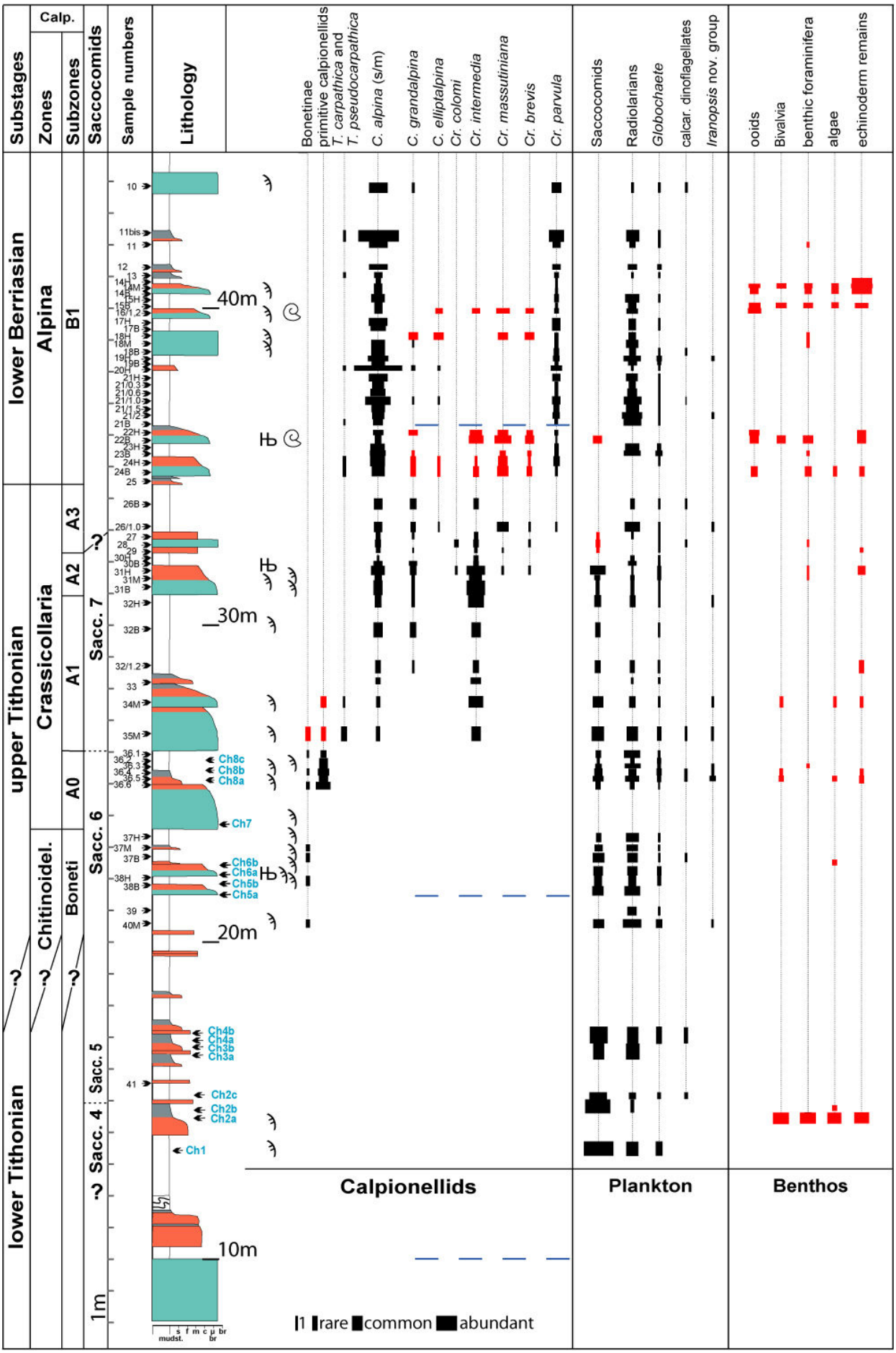
Substages
Zones
Subzones
Saccocomids
Sample numbers
Lithology
lower Berriasian
upper Tithonian
lower Tithonian
Alpina
Crassicollaria
Chitinoidel.
Boneti
Calp.
B1
A3
A2
A1
A0
Sacc. 7
Sacc. 6
Sacc. 5
Sacc. 4
40m
30m
20m
10m
1m
Ch8c
Ch8b
Ch8a
Ch7
Ch6b
Ch6a
Ch5b
Ch5a
Ch4b
Ch4a
Ch3b
Ch3a
Ch2c
Ch2b
Ch2a
Ch1
Bonetinae
primitive calpionellids
T. carpathica and
T. pseudocarpathica
C. alpina (s/m)
C. grandalpina
C. elliptalpina
Cr. colomi
Cr. intermedia
Cr. massutiniana
Cr. brevis
Cr. parvula
Saccocomids
Radiolarians
Globochaete
calcar. dinoflagellates
Iranopsis nov. group
ooids
Bivalvia
benthic foraminifera
algae
echinoderm remains
Calpionellids
Plankton
Benthos
rare
common
abundant
mudst.
s f m c μ br

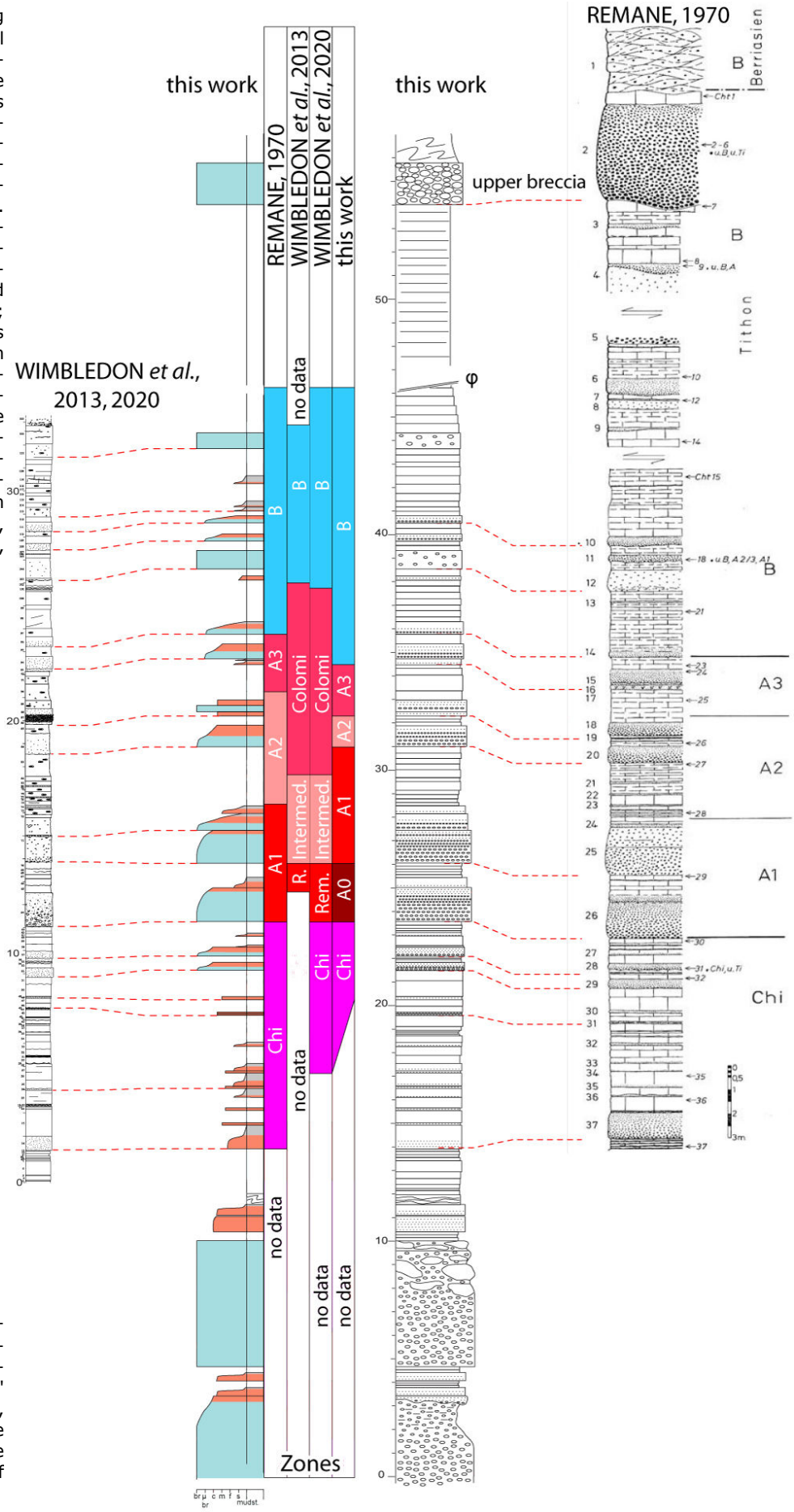

◀ **Figure 2:** Le Chouet log displaying the lithological succession, the stratigraphic distribution of the main (micro-) fossil groups of the Tithonian-lower Berriasian, both the calpionellid and saccocomid biozones, and the main reworked neritic elements. Autochthonous sedimentation (mud- and wackestones) is in white; cryptoturbidites (micropack- and micrograinstones) in grey; coarse grained turbidites (pack- and grainstones) in orange; debris flows (float- and rudstones) in blue-green. The red color in the distribution columns corresponds to reworked material. Ⱨ: belemnite rostrum; ⅄: aptychus; grain size: s, silt; f, m, c, fine, medium, coarse sands; μbr, microbreccia; br, breccia.

▶ **Figure 3:** Lithostratigraphic correlations of REMANE's 1970 log (right column), WIMBLEDON *et al.*' 2013 log (left column), and this study (center; see caption in Fig. 2) with the various interpretations of the calpionellid biozones.

Figure 4: Lower (I) and upper (A-H) Tithonian facies. A: pinkish cryptoturbidites 25; B: breccia 28 sandwiched between turbidites 27 (above) and 29 (below); C: breccia 35 and its basal erosion surface; D: breccia Ch7 and its basal erosion surface; E: breccia Ch7 (top) and graded turbidites Ch6 and Ch5 (bottom); F: enlargement of E, detail of the basal erosion surface of the graded turbidite Ch6; G: enlargement of E, detail of the graded turbidite Ch5; H: basal erosion surface of the turbidite 40; I: thin cryptoturbidite Ch4 with a silty beige base (m) indicating a faint grading. A, F-G, I: pencil for scale; B, D: JACOB's staff for scale; C, E: no physical scale; H: finger for scale.

2. Studied section

The Le Chouet section is located some tens of meters southeast of the eponymic farm (Les Près municipality, La Drôme department, Fig. 1), in an area located in the center of the geological map at 1/50,000 scale of Luc-en-Diois (FLANDRIN, 1970). A composite section, more than 50 m long (Figs. 2-3), was measured along the tarred track from the D306 departmental road to the Le Chouet farm. It is split in three parts: 1) The lower part, which is sited on the left side of the stream, starts after a short tunnel section (GPS coordinates: 44°32'25.8"N 5°33'37.4"E). It corresponds to the first 10 m of the logged section. 2) The median part starts at the hairpin bend (GPS coordinates: 44°32'34.3"N 5°33'37.0"E) where the track crosscuts the Fournet stream, one of the small tributaries of La Drôme river. This median part, which is sited on the right side of the stream, ends with a fault at 46 m height on the log (GPS coordinates: 44°32'29.7"N 5°33' 32.5"E). The outcrop conditions after the fault become poor; consequently, 3) the upper part of the section was not logged in detail. The whole section (Figs. 2-3) was measured with a JACOB's staff and later correlated with those of REMANE (1970: Fig. 6) and WIMBLEDON *et al.* (2013: Fig. 4, 2020a: Supplement Fig. S1): Figure 3. An eight meter offset exists between the log on Figure 2 and that on Figure 3 ; we shall refer to Figure 2 to give the elevations of the beds and samples on the logged section.

3. Material and methods

The Le Chouet section was sampled twice, the first 16 samples with labels ranging from Ch1 to Ch8c (collected on the occasion of a first visit on 2018/05/08 by the second author, S.F., see Fig. 2) and the second 64 samples with labels ranging from 41 to 10 (collected on the occasion of a second joint visit on 2019/05/12 by the first author, B.R.C.G, and the second author, S.F., see Fig. 2). The rock samples were cut and the derived slabs scrupulously examined in the search for mud turbidites, grainy turbidites and debris flows. In addition, sets of thin sections were successively prepared to validate the identification of mud turbidites, identify the source of the lithoclasts (parautochthonous or allochthonous), and study the microfossil contents.

4. Lithostratigraphy

4.1. Summary description

The lower part (up to 2 m on Fig. 2) is comprised of two massive breccia intervals of the uppermost Tithonian breccia. In the next interval (up to 14 m on the log of Fig. 2) the yellowish to light grey limestones that form the "background" basinal sedimentation are irregularly alternating with thin beds of fine-grained (Fig. 4H) to mud (Fig. 4I) turbidites. From 14 upward to 28 m on the same log, thick beds made of coarse-grained graded turbidites (Figs. 4B *pars*, C, E *pars*, F-G, 5G-I) and breccias, often rudstones of pebbles and cobbles (Fig. 4B *pars*, D, E *pars*), are common whereas the mud turbidites remain present (Figs. 4A, 6L). The facies of the next and last interval, up to the fault (at 38 m), are characteristic of the "calcaires blancs" (white limestones) and include some cryptic mud turbidites (Fig. 5B). Additionally, this interval still displays graded turbidites (Fig. 5C-D, F *pars*) and breccias, often floatstones of pebbles and cobbles (Fig. 5A, E).

4.2. Macrofacies and microfacies

In terms of macro- and microfacies, the rocks naturally fall into two categories: 1) the autochthonous facies and 2) the parautochthonous- and allochthonous-derived facies.

The first category corresponds to background facies related to the regular sedimentation of pelagic material falling and slowly accumulating on the seafloor. They consist of mud- and wackestone microfacies with saccocomids (which are here restricted to Tithonian strata), calpionellids (which are here restricted to upper Tithonian - lower Berriasian strata), and/or radiolarians (which may occur here in both Tithonian and lower Berriasian strata). Besides the pelagic groups of microorganims, which also comprise calcareous dinoflagellates (Fig. 7AH-AJ), *Globochaete alpina* LOMBARD (Figs. 6G, 7Y-AB) and the *Iranopsis* nov. group (Fig. 7AC-AG, AK-AN), the thin sections contain various parautochthonous and autochthonous bioclasts, either smaller (*e.g.*, sponge spicules) or larger ones [*e.g.*, aptychii (Fig. 6O), ammonite phragmocones (Fig. 6M *pars*), belemnite rostra (Fig. 6N) and jaws].

The second category corresponds to gravity-flow deposition in the form of turbidites and associated debris flows. They consist of pack- and grainstones that commonly form the matrices of lithoclastic float- and rudstones. Basal surfaces of both turbidites and debris flows are commonly erosional (Fig. 8). Some lithoclasts have been created by the erosive processes that have affected more or less deeply the underlying strata. Subsequently they were incorporated into the turbidites and debris flows. These lithoclasts are not intraclasts, but pseudointraclasts, because they do not result from the *in situ* dismantling of the same and single layer but that of several discrete layers located updip on the slope. Accordingly, a single breccia layer contain several discrete types of pseudointraclasts (*e.g.*, saccocomid wackestone lithoclasts, calpionellid wackestone lithoclasts, radiolarian wackestone lithoclasts, and even microlithoclastic grainstone lithoclasts). GRANIER *et al.* (2020b) referred to them as "extraclasts" whereas GRANIER *et al.* (2023) identified them as "pseudointraclasts" because their fabrics are similar to that of the background relatively deep-water sedimentation in contrast to the extraclasts *sensu stricto* that correspond to lithoclasts reworked from updip shallow-water areas.

Figure 5: Berriasian facies. A: floatstone breccia 10; B: pinkish cryptoturbidites 12 (m); C: graded turbidite 14; D: graded turbidite 16; E: enlargement of F, detail of floatstone breccia 18; F: turbidite 20 (bottom) and floatstone breccia 18 (top); G: graded turbidite 22; H: graded turbidite 24 (above) eroding fine-grained turbidite 25 (below); I: enlargement of H, detail of the contact of turbidites 25 (below) and 25 (above). A-B, D, F, I: hammer for scale; C, E: pencil for scale; H: no physical scale.

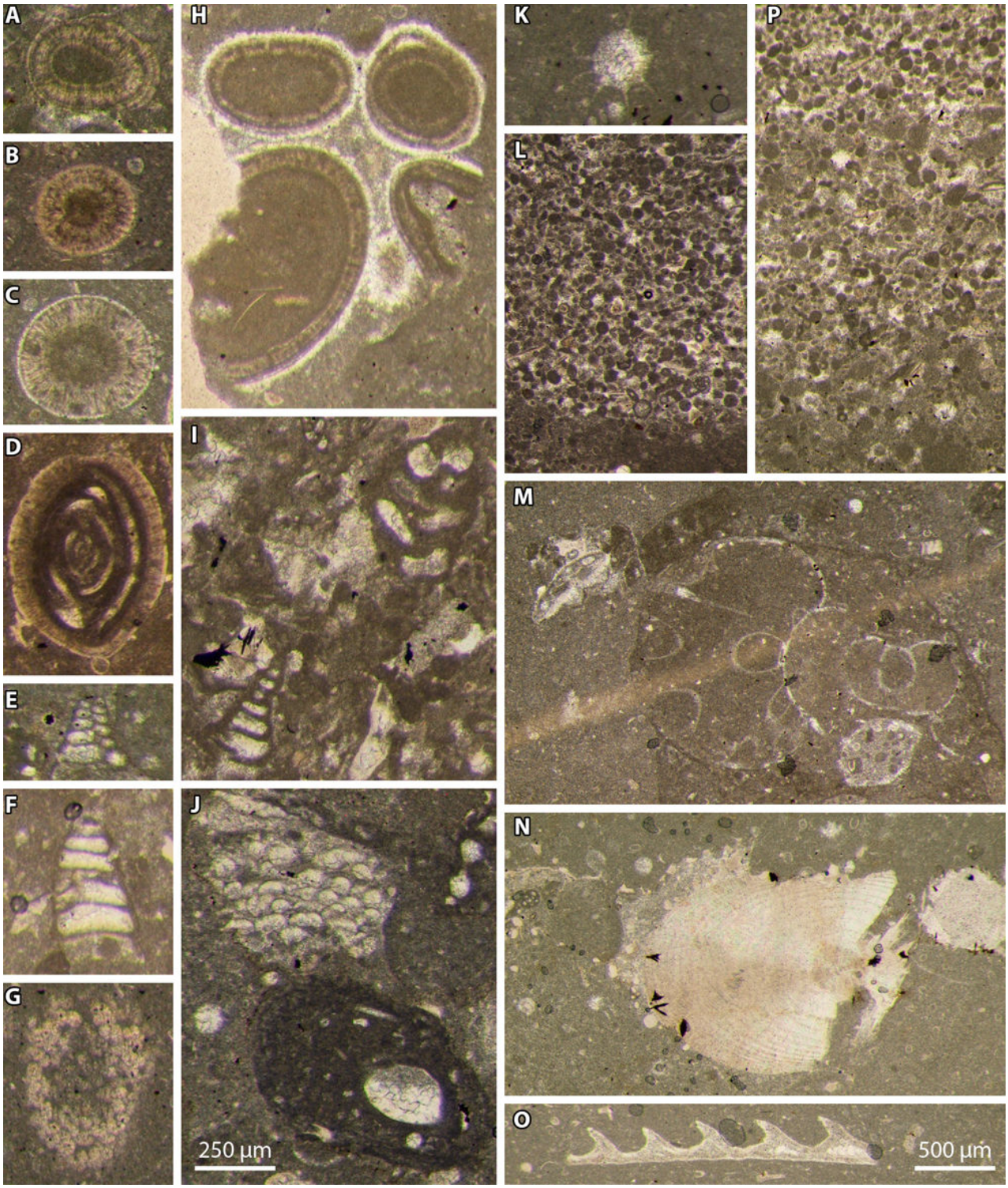

Figure 6: Reworked and *in situ* material from Le Chouet section. A-D: concentric radial ooids (a miliolid as a nucleus in D); E-F: biseriate foraminifers, Textulariidae; G: set of *Globochaete alpina* LOMBARD on a lamella (tangential section); H: extraclast of oolitic grainstone, reworked from a hardground as evidenced by its early marine fibrous cementation; I: *Redmondoides lugeoni* (SEPTFONTAINE) at the top and a biseriate foraminifer (Textulariidae) at the bottom; J: *Koskinobullina socialis* CHERCHI & SCHROEDER at the top and *Tubiphytes* sp. at the bottom; K: *incertae sedis*; L: erosional surface at the bottom of a micrograinstone ("mud turbitidite", cryptoturbidite) with numerous calpionellid loricae in microlithoclasts; M: *Mohlerina basiliensis* (MOHLER) at the left top and ammonite phragmocone in transverse section to the right; N: belemnite rostrum; O: aptychus; P: micrograinstone (fine-grained turbidite) with numerous calpionellid loricae in microlithoclasts. Photomicrographs A-K, N with the same scale (scale bar on J = 250 µm), photomicrographs L-M, O-Q with the same scale (scale bar on O = 500 µm). A: sample 14B; B, H: sample 15B; C: sample 34M; D: sample Ch8a; E, J: sample Ch6b; F, I: sample Ch8b; G: sample 31M; K: sample 40M; L: sample 30H; M: sample 16; N: sample 14M; Q: sample 22B; O: sample 31H; P: sample 25. Upper Tithonian: C-G, I-L, O; lower Berriasian: A-B, H, M-N, P.

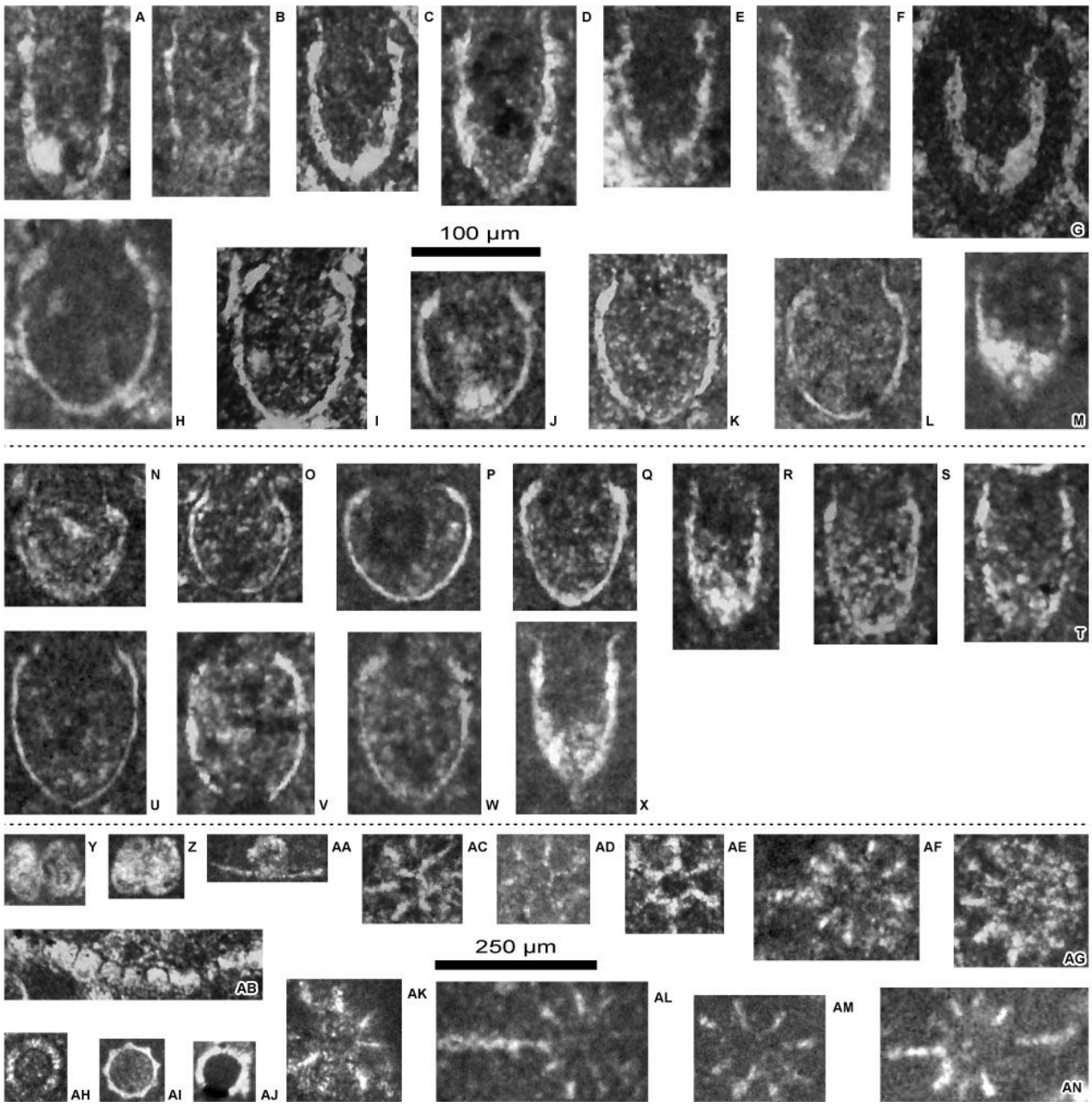

Figure 7: A-X: Calpionellid specimens from the Crassicollaria Zone (A3 subzone) and the Alpina Zone (B1 subzone) - reworked and/or *in situ* material - of the Le Chouet section. A-M: Brevis-Massutiniana Subzone (A3 subzone), N-T: Alpina-Parvula Subzone (B1 subzone), U-X: specimens from the top of the Crassicollaria Zone reworked in the Alpina-Parvula Subzone (B1 subzone). A-D: *Crassicollaria massutiniana* (COLOM) (reworked specimens); E-G: *Cr. brevis* REMANE (reworked specimens; G: specimen in a microlithoclast); H: *Calpionella grandalpina* NAGY (reworked specimen); I: *C. elliptalpina* NAGY (reworked specimen); J: small-sized *C. alpina* LORENZ (reworked specimen); K-L: medium-sized *C. alpina* LORENZ (reworked specimens); M: *Tintinnopsella pseudocarpathica* BENZAGGAGH *et al.* (reworked specimen); N-P: *Calpionella alpina* LORENZ with ovoid rounded loricae; Q: *C. alpina* LORENZ with ovoid elongated lorica; R-T: *Crassicollaria parvula* REMANE; U-W: *Calpionella elliptalpina* NAGY (reworked specimens); X: *Crassicollaria intermedia* DURAND DELGA (reworked specimen). Y-AN: Various microfossils from Tithonian - lower Berriasian of the Le Chouet section. Y-AB: *Globochaete alpina* LOMBARD: Y-Z, as pairs; AA, isolated on a lamella; AB, set on a lamella (transverse section); AC-AG, AK-AN: *Iranopsis* nov. group; AH: *Colomisphaera carpathica* (BORZA); AI: *Parastomiosphaera tuberculata* BENZAGGAGH *et al.*; AJ: *Parastomiosphaera* aff. *malmica* (BORZA). Photomicrographs A-Z with the same scale bar = 100 µm, photomicrographs Y-AN with the same scale bar = 250 µm. A-B, D, AA: sample 22B; C, E-I, K, AB: sample 24B; J, L: sample 23H; M: sample 22H; N-O: sample 10; P: sample 18M; Q: sample 19B; R: sample 15H; S-T: sample 21B; U: sample 18M (reworked specimen); V: sample 21/1.0; W: sample 21B (reworked specimen); X: sample 16/1.2 (reworked specimen); Y, AM-AN: sample 36.5; Z: sample 36.4; AC: sample 40M; AD, AI, AL: sample 26/1.0; AE: sample 38B; AH: sample 18B; AF, AK: sample 19H; AG: sample 21/2.0; AJ: sample Ch2a. Lower Tithonian: AJ; upper Tithonian: Y-Z, AC-AE, AI, AL-AN; lower Berriasian: A-X, AA-AB, AF-AI, AK-AL.

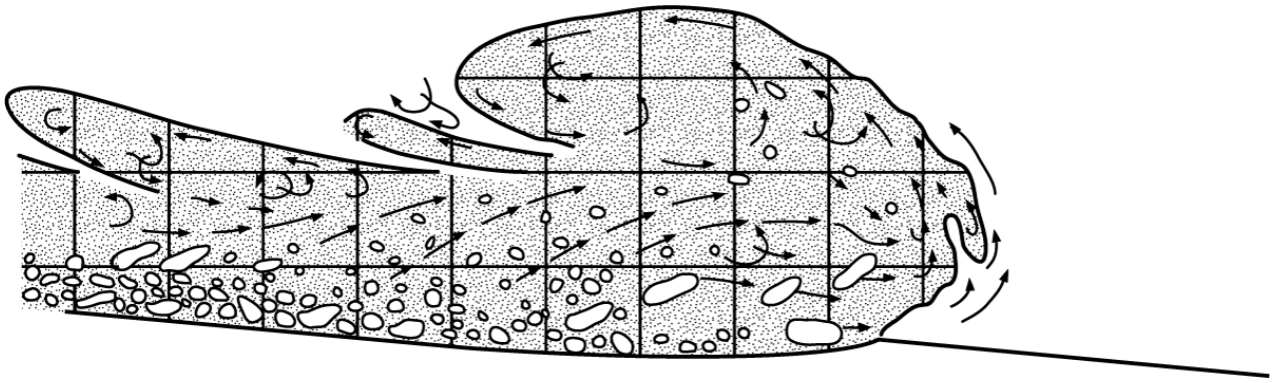

Figure 8: Avalanche model for the formation of debris flows and related calciturbidites combining erosion and transportation modified from POSTMA *et al.* (1988).

The pseudointraclasts are usually larger and subrounded (Fig. 9B, D-G) because they were made of mechanically abraded unlithified material whereas the extraclasts *sensu stricto* are commonly smaller and subangular (Figs. 6H, 9A, C, H). Extraclasts *sensu stricto* but also skeletal grains (bioclasts) and concentric calcitic ooids (Fig. 6A-D, N *pars*) are all reworked from shallow-water environments of a neighbouring platform edge. For instance, these extraclasts may consists of cemented oolitic grainstones (Fig. 9C) or of microbial boundstones. Bioclasts are diverse comprising bryozoans, calcareous and siliceous sponges, hermatypic corals (Fig. 9A), echinoderm remains, calcareous algae [among which *Salpingoporella pygmaea* (GÜMBEL) (Fig. 10F), *S. annulata* CAROZZI (Fig. 6N *pars*) and *Thaumatoporella parvovesiculifera* (RAINERI) (Fig. 11A-E), as well as the problematic *Iberopora bodeuri* GRANIER & BERTHOU (Fig. 10S-U)], and foraminifers. The benthic foraminifers are the most diverse: ataxophragmiids (Fig. 12AH-AJ), *Redmondoides lugeoni* (SEPTFONTAINE) (Fig. 6I *pars*), textulariids (Fig. 6E-F, I *pars*), lituolids (Fig. 10N-R, V), miliolids (Fig. 6D), lenticulinids, *Frentzenella* sp. (Fig. 11R-T), *Coscinoconus* sp. (Fig. 10A-F), *Ichnusella* spp. (Fig. 12A-AB), *Mohlerina basiliensis* (MOHLER) (Figs. 6M *pars*, 10J-M, 11O-Q, U), *Protopeneroplis ultragranulata* (GORBATCHIK) (Fig. 12AC-AF, ?AG), as well as the incertae sedis *Koskinobullina socialis* CHERCHI & SCHROEDER (Fig. 6J *pars*) and *Tubiphytes* sp. (Figs. 6J *pars*, 9H).

As in the Tré Maroua section (GRANIER *et al.*, 2020b, 2023), the Le Chouet section contains a number of cryptoturbidites, *i.e.*, well-sorted micrograinstones with a very finely lithoclastic composition. These mud turbidites are hardly detectable with hand lenses in the field (GRANIER *et al.*, 2020b, Fig. 5). Their nature is fully revealed only with thin sections under a standard microscope (Fig. 6L, P). WIMBLEDON *et al.* (2013, Fig. 8.2-4, 8.6) have identified similar microfacies as pelbiomicrosparites or pelbiosparites. As a matter of fact, most allochems that are less than 100 µm in diameter are not bioclasts or peloids but mostly small rounded pseudointraclasts (microlithoclasts, Fig. 6L, P), commonly consisting of a calpionellid lorica filled and coated by micrite.

5. Biostratigraphy (M.B.)

5.1. Saccocomid biozones: For practical reasons, saccocomid sections have been named after their geometric shapes (BENZAGGAGH *et al.*, 2015) as follows: 2Ax.act.br: biaxis with acute branches; 2Ax.brd.br: biaxis with broad branches; 2prl.Br: two parallel branches; 2tn.prl.Br: two thin parallel branches; 3Ax.act.br: triaxis with acute branches; 3Ax.brd.br: triaxis with broad branches; brd.2Ax: broad biaxis; brd.ml.Tt: broad molar tooth thin; cnc.ml.Tt: concave molar tooth; cvx.ml.Tt: convex molar tooth; div.elg.Br: divided elongated branch; elg.Br: elongated branch; elg.ml.Tt: elongated molar tooth; elg. psd-hxg.Hd: elongated pseudo-hexagonal head; elg.Tt: elongated tooth; flt.psd-hxg.Hd: flattened pseudo-hexagonal head; irg.Hd: irregular head; prp.Wg: propeller wings; srd.Wg: serrated wings; tn.Wg: thin wings; /2lat.apd:with two lateral appendices; /ax.tp: with axial tip; /elg.ax.tp: with elongated axial tip; /elg.tp: with elongated tips; /int.cvt: with internal cavity; /ov.ax.tp: with ovoid axial tip; /psd-rtg.ax.tp: with pseudo-rectangular axial tip; /ptd.bs: with pointed basis; /shr.ax.tp: with short axial tip; /smpl.tp: with simple tips; /tk.ts: with thick test; /tn.crw: with thin crown; /tn.flt.crw: with thin and flat crown; /trg.cvt: with triangular cavity.

This microfossil group largely dominates the pelagic assemblages of the Tethys realm at least from the earliest Tithonian (Hybonotum Zone) up to its disappearance in the latest Tithonian. However, it has been largely overlooked except in the outer Rif of Morocco. Five saccocomid zones (zones 3-7) have been defined for the Tithonian stage (BENZAGGAGH *et al.*, 2015: Fig. 17). Four of them, *i.e.*, the saccocomid zones 4 to 7, are identified in the Le Chouet section. The assemblages and successions at Le Chouet are very similar to those known in the outer Rif with a large dominance of thick sections in the lowermost Tithonian (Saccocomid zone 4), with highly diversified smaller sections in both the upper lower Tithonian (Saccocomid zone 5) and the lower upper Tithonian (Saccocomid zone 6), and finally with less frequent and undiversified sections dominated by biaxial sections in the middle upper Titho-

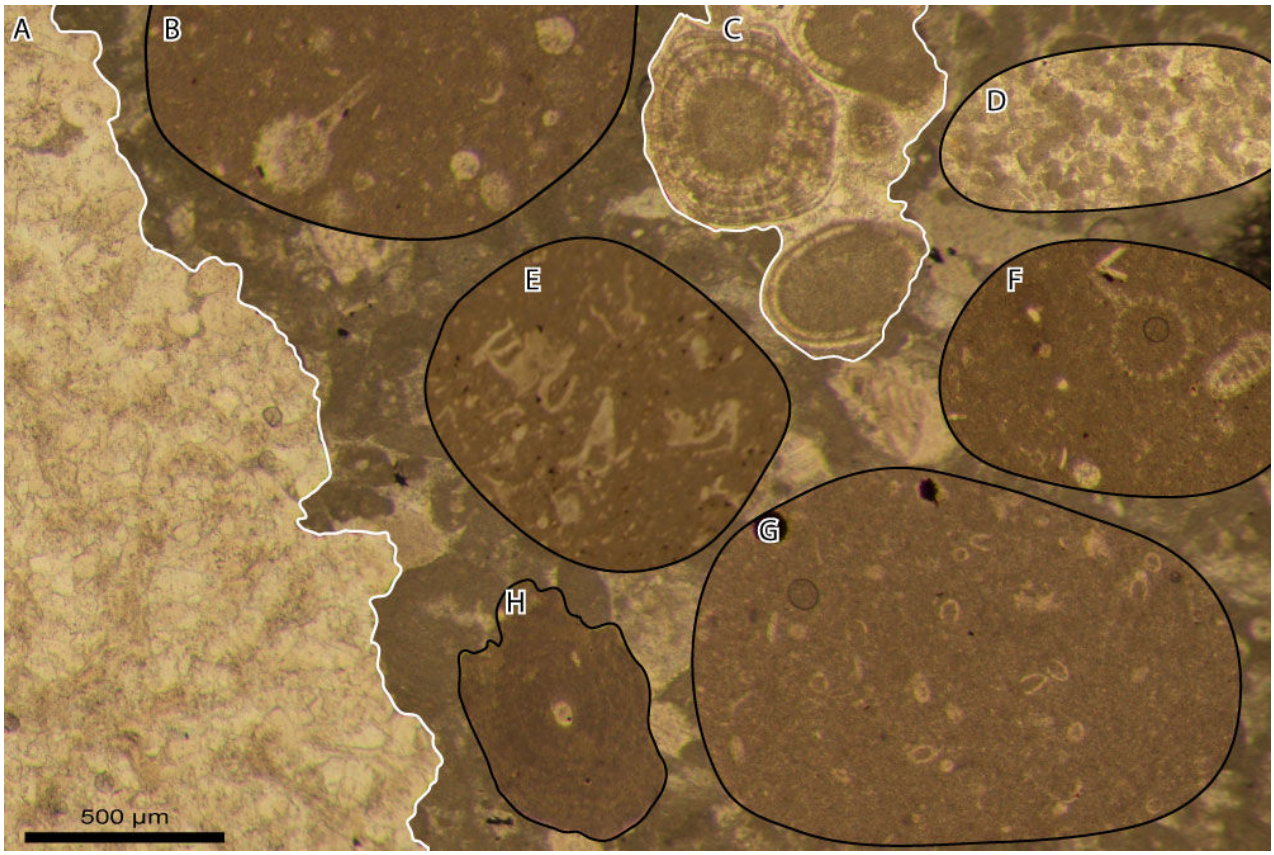

Figure 9: Composite* debris flow microfacies. A: extraclast of hermatypic coral boundstone; B, F: extraclast of radiolarian wackestone; C: extraclast of oolitic grainstone; D: extraclast of microclastic grainstone (turbidite) with calpionellids; E: extraclast of saccocomid wackestone; G: extraclast of calpionellid wackestone; H: *Tubiphytes* sp. The matrix is a bioclastic and extraclastic (pack-) grainstone. The lithoclasts B and D-G, which should be derived from slope and/or basinal facies, are also referred to as pseudointraclasts. *: The background as well as clasts B and D-F are patches copied from another source and pasted here to illustrate a perfect example of calcareous debris flow (if all types of clasts may well occur in the same thin section, they hardly occur in the same field of view). The background is derived from thin section Ch8b-2 whereas the fake clast B is derived from 37H, D from 11, E from Ch1, and F from 34M. Genuine clast A is observed in thin section Ch6 whereas C is found in 14B, G in 18H, and H in Ch8b-2. All photomicrographs with the same bar = 500 µm.

nian (Saccocomid zone 7). In the Le Chouet section, samples Ch1-Ch2b contain numerous saccocomid sections (Fig. 13A-CD) dominated by large and thick forms (Fig. 13A-D, F-G). The latter become scarcer in samples Ch3a-Ch4b with an assemblage dominated by sections typical of the upper lower Tithonian (Fig. 13E, H-T). In the overlying samples (40M to 27), saccocomid sections become less and less abundant and are dominated by smaller forms (Fig. 13U-CD). The group disappears at the base of the Crassicollaria subzone A3 above sample 27. Note that samples 29-27 were picked in a turbiditic interval and these specimens are possibly reworked. Sample 22B picked in the second debris flow level above the base of the calpionellid zone B (*i.e.*, the former Tithonian/Berriasian boundary) also contains some reworked specimens.

5.1.1. Saccocomid zone 4 (equivalent to the Darwini and Semiforme zones, above the Hybonotum Zone) is characterized by an abundance of thick sections of the srd.Wg/tk.ts, irg.Hd, and flt.psd-hxg.Hd/2lat.apd types. At the base of the Le Chouet section (Ch1 and Ch2a-b), the typical saccocomid sections of the zone 3 are missing and these levels are ascribed to the saccocomid zone 4. The assemblage is dominated by large and thick sections, *e.g.*, irg.Hd (Fig. 13A-C, H), th.Wg/ov.ax.tp (Fig. 13D, F), and th.Wg/shr.ax.tp (Fig. 13G). It also comprises sections of the 2Ax. act.br/ptd.bs (Fig. 13E, R), flt.psd-hxg.Hd/2lat. apd (Fig. 13N), 2prl.Br/elg.tp (Fig. 13M), div.elg. Br (Fig. 13I-J, LF), elg.Tt (Fig. 13T), and cvx.ml. Tt/lrg.crw (Fig. 13P) types.

5.1.2. In contrast to the previous zone, **Saccocomid zone 5** (equivalent to the Fallauxi Zone) is characterized by the scarcity of thick sections and by the relative abundance of far less thick sections of the elg.psd-hxg, flt.psd-hxg.Hd, elg.Br, 2prl.Br/smpl.tp, 3Ax.brd.br, tn.Wg, elg.Tt, ml.Tt, and 2Ax.brd.br/elg.ax.tp types. In levels Ch2a to Ch4b, the saccocomid assemblage is dominated by sections of the div.elg.Br (Fig. 13Q), elg.Tt (Fig. 13K, S), and cvx.ml.Tt /lrg.crw (Fig. 13O) types.

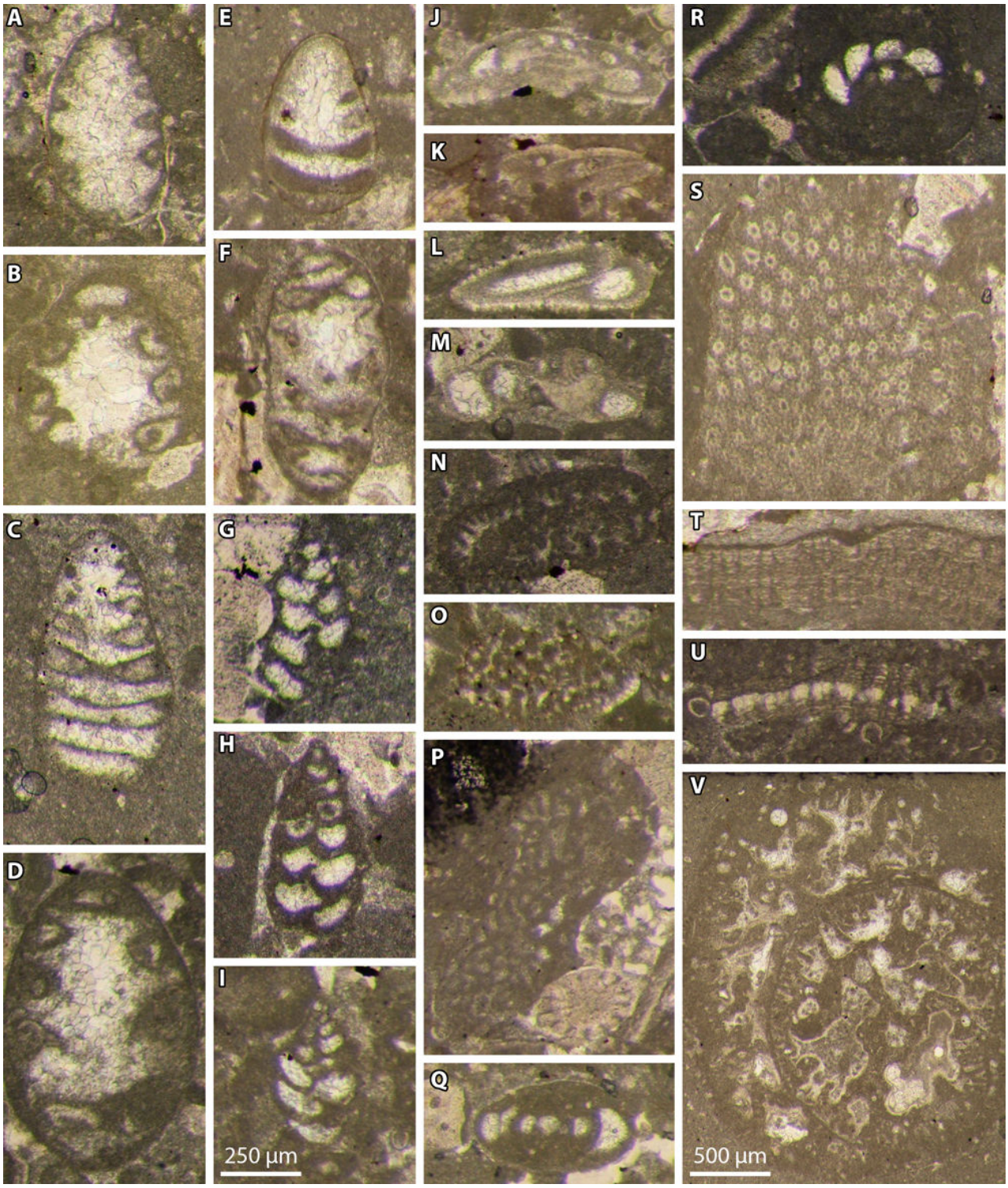

Figure 10: Reworked benthic foraminifers and calcareous algae from Le Chouet section. A-F: *Coscinoconus* sp.; G-I: ? Ataxophragmiidae; J-M: *Mohlerina basiliensis* (MOHLER); N-O: cf. *Anchispirocyclina lusitanica* (EGGER); P: sea urchin radiole (bottom right) and subepidermal meshwork of a large agglutinated foraminiferal test; Q-R: *Nautiloculina* sp.; S-U: *Iberoporella bodeuri* GRANIER & BERTHOU, with *Calpionella alpina* in U; V: large agglutinated foraminiferal test. All photomicrographs with the same scale (scale bar on R = 250 µm). A-B, L, S: sample 14B; C: sample 18H; D, I-K, M, U: sample Ch8b; E: sample 22M; F: sample 14M; G: sample 15B; H: sample Ch2a; N-O: sample Ch6b; P-R: sample Ch8a; T: sample 24B; V: sample 16. Lower Tithonian: H; upper Tithonian: D, I-K, M-R, U; lower Berriasian: A-C, E-G, F, S-T, V.

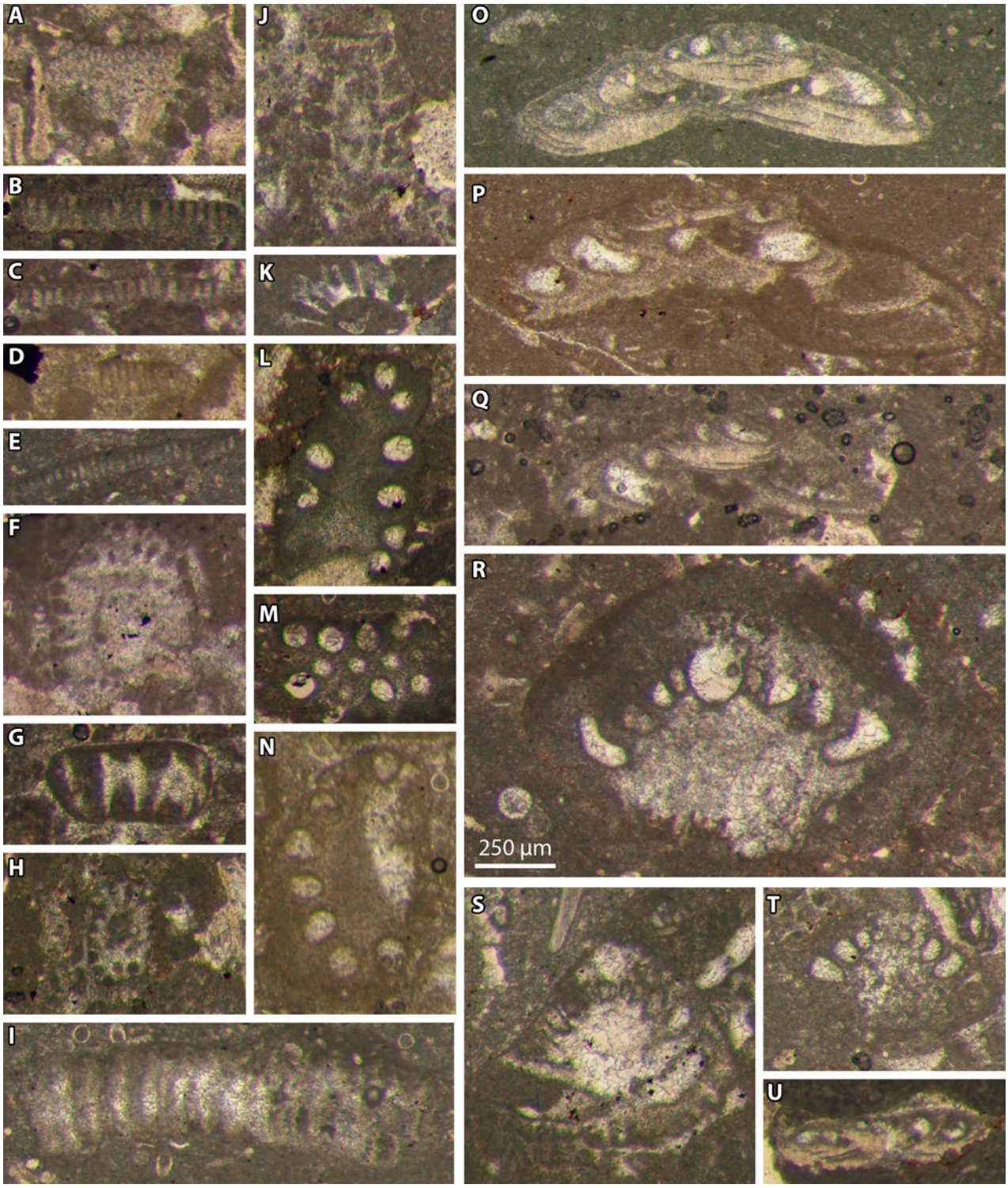

Figure 11: Reworked calcareous algae, sponges, and benthic foraminifers from Le Chouet (A-M, O-U) and Tré Maroua (N) sections. A-E: *Thaumatoporella parvovesiculifera* (Raineri); F-H, ?I: *Salpingoporella* sp. [F: *S.pygmaea* (Gümbel)]; J-K: ? *Clypeina* sp.; L-N: *Perturbatacrusta leini* Schlagintweit & Gawlick, 2011; O-Q, U: *Mohlerina basiliensis* (Mohler); R-T: *Ichnusella* sp.. All photomicrographs with the same scale (scale bar on R = 250 µm). A: sample Ch2b; B, H, J, L: sample Ch6b; C-D, G: sample Ch8b; E, T: sample 14B; F: sample 14M; I: sample 15B; K, R: sample Ch6a; M, S: sample Ch8a; N: Tré Maroua 58; O: sample 31M; P: sample 16; Q: sample 22M; U: sample 22b. Lower Tithonian: A; upper Tithonian: B-D, G-H, J-M, O, R-S; lower Berriasian: E-F, I, N, P-Q, T-U.

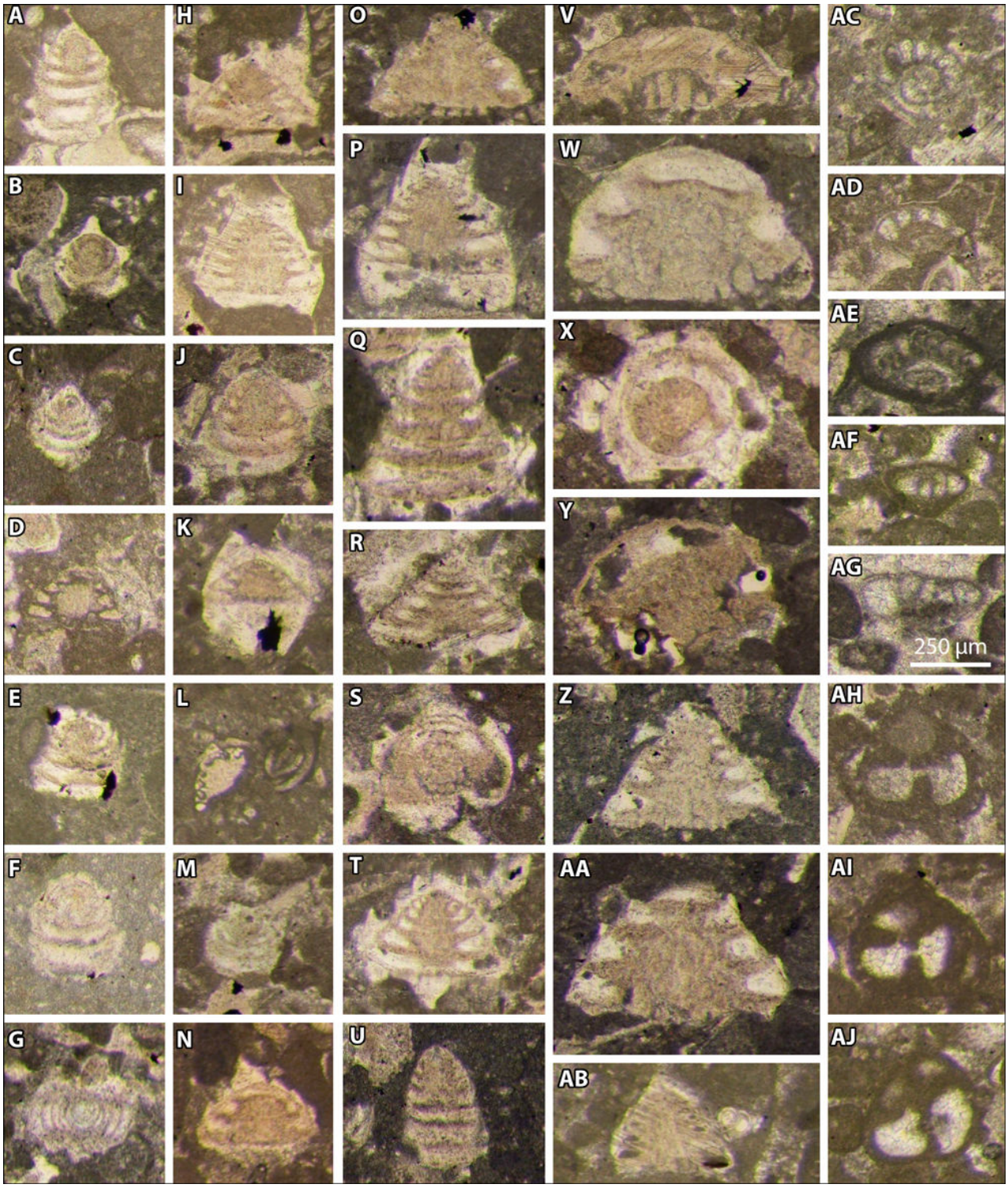

Figure 12: Reworked benthic foraminifers from Le Chouet section. A-AB: *Ichnusella* spp. including *Ichn. infragranulata* (NOTH); AC-AF, ?AG: *Protopeneroplis ultragranulata* (GORBATCHIK); AH-AJ: triseriate foraminifers, Ataxophragmiidae. All photomicrographs with the same scale (scale bar on AG = 250 µm). A, I: sample 14B; B, U, AA: sample Ch8a; C-D, H, S-T: sample 14M; E: sample 15B; F: sample 22B; G, AC: sample Ch2b; K-Q, V, X-Y, AB, AD-AE, AH-AJ: sample Ch8b; R, W, Z: sample Ch6b; AF-AG: sample 24B. Lower Tithonian: G, AC; upper Tithonian: B, K-R, U-AB, AD-AE, AH-AJ; lower Berriasian: A, C-F, H-I, S-T, AF-AG.

5.1.3. Saccocomid zone 6 (equivalent to the Ponti Zone and, *pro parte*, the Microcanthum Zone) is rich in sections of tn.Wg, prp.Wg, elg.psd-hxg, 2prl.Br, 2tn.prl.Br, 3Ax.brd.br, 2Ax.brd.br/trg.cvt/ax.tp, elg.Br, 2Ax.brd.br, and elg.Tt types, as well as the various sections of the ml.Tt type. In the Le Chouet section, the assemblage of samples 40M-36.1 is composed of sections of tn.Wg/shr.ax.tp (Fig. 13BX, BZ), flt.psd-hxg.Hd/2lat.apd (Fig. 13CA-CB), elg.psd-hxg.Hd/2lat.apd (Fig. 13CC), 2tn.prl.Br (Fig. 13BW), brd.2Ax/trg.cvt (Fig. 13BK), 2Ax.brd.br/trg.cvt/ax.tp (Fig. 13BB), 2prl.Br/elg.tp (Fig. 13BY), 3Ax.brd.br (Fig. 13BD, BF-BG), and 2Ax.act.br/ptd.bs (Fig. 13AN) types, as well as frequent sections of 2Ax.brd.br/rd.ax.tp (Fig. 13U1, X-Y1, W, AB, AD-AE, AL, AP, AU, AW), 2Ax.brd.br/psd-rtg.ax.tp (Fig. 13U2, Y2, AO, AR-AS, AV, AX-AY), 2Ax.brd.br/shr.ax.tp (Fig. 13AI, AK, AT), 2Ax.brd.br/elg.ax.tp (Fig. 13AF), cnc.ml.Tt (Fig. 13BN-BQ, BT), cvx.ml.Tt/tn.crw/int.cvt (Fig. 13BS), elg.ml.Tt/tn.flt.crw (Fig. 13BL), and elg.Br (Fig. 13BU) types.

5.1.3. Saccocomid zone 7 (equivalent to the upper part of the Microcanthum Zone and the lower part of the Durangites Zone) contains fewer saccocomid sections. Its assemblage is largely dominated by sections of 2Ax.brd.br type, with a rounded (Fig. 13AA, AC, AG-AH, AM, BE), elongated (Fig. 13BI) or pseudo-rectangular (Fig. 13V, Z, AQ) axial apex, and it contains rare sections of 3Ax.brd.br, elg.Br, 2prl.Br/smpl.tp, tn.Wg, 2Ax.brd.br/trg.cvt/ax.tp (Fig. 13AZ, BA), elg.Tt, and ml.Tt types. At Le Chouet, it also contains common 2Ax.brd.br/trg.cvt/ax.tp type and rare sections of cnc.ml.Tt (Fig. 13BM), brd.ml.Tt/tn.flt.crw (Fig. 13BR), flt.psd-hxg.Hd/2lat.apd (Fig. 13CD), 3Ax.brd.br (Fig. 13BC, BH), and div.elg.Br (Fig. 13BV) types.

5.2. Chitinoidella Zone (Boneti Subzone): Contrary to the Dobeni Subzone that to date has never been identified in any of the Vocontian Trough sections, the Boneti Subzone is characterized here by the occurrence of species belonging exclusively to the subfamily Bonetinae (Fig. 14A-F), the assemblage of which is similar to those known from both margins of the Tethys realm (*i.e.*, eastern and western Europe, Turkey, Iran, Cuba, Mexico, and recently reported from the Blue Nile Basin in Ethiopia, JAIN *et al.*, 2021) and outside it (*e.g.*, in the Neuquén basin of the eastern Pacific margin of Argentina, KIETZMANN, 2017; KIETZMANN *et al.*, 2021). In the Ardescian series, CECCA *et al.* (1989) have already reported the occurrences of "*Chitinoidella* sp.", "*Ch. boneti* DOBEN", and "*Ch.* cf. *cubensis* (FURRAZOLA-BERMÚDEZ)" whereas, in the Le Chouet section, samples 40M-37M contain *Bonetilla boneti* (DOBEN) (Fig. 14A), *Furrazolaia insueta* (ŘEHÁNEK) (Fig. 14B), and *F. cristobalensis* (FURRAZOLA-BERMÚDEZ) (Fig. 14C-D). Due to a discontinuous sampling from Ch4b to 40M, *i.e.*, a nearly 5 meter interval, the base of the Boneti Subzone could not be accurately defined.

5.3. Calpionellid zones (BENZAGGAGH, 2020)**:** Close-spaced sampling of the Le Chouet section allowed characterization of the four subzones of the Crassicollaria Zone and the first subzone of the Alpina Zone. The first specimens of calpionellids with microgranular loricae are reported from sample 40M whereas the first specimens of calpionellids with hyaline tests appear in sample 36.6. The latters are represented by primitive, often small loricae with undeveloped or poorly developed collars (Fig. 14G-X). They are initially sparse to moderately abundant but they become abundant and dominate the pelagic microorganisms from the upper half of the upper Tithonian Crassicollaria Zone and throughout the lower Berriasian Alpina Zone.

5.3.1. Crassicollaria Zone (zone A): In the Vocontian Basin, as in most basins of the Tethys margins, the Crassicollaria Zone is dominated by the genus *Crassicollaria*. In the Le Chouet section, it spans the interval ranging from sample 36.6 (and probably Ch7) to sample 26B. Its base is marked by an interval containing the last chitinoidellids and the first primitive calpionellids (subzone A0), equivalent to the Remanei and Praetintinnopsella zones of some authors (*e.g.*, REMANE *et al.*, 1986; ÖLVECZKÁ & REHÁKOVÁ, 2022). The rest of the zone is subdivided into three successive assemblage subzones with from bottom to top: 1) one with numerous small to medium-sized *Crassicollaria intermedia* and some *Calpionella grandalpina* (subzone A1), 2) another with numerous regular *Crassicollaria intermedia*, larger in size than those of the underlying subzone, and with few *Cr. colomi*

▶ **Figure 13:** Sections of skeletal segments of Tithonian saccocomids from the saccocomid zones 4 to 7 in the Le Chouet section. A-C, H: irg.Hd; D, F: th.Wg/ov.ax.tp; E, R, AN: 2Ax.act.Br/ptd.bs; G: th.Wg/shr.ax.tp; I-J, L, Q: div.elg.Br; K, S-T: elg.Tt; M: 2prl.Br/elg.tp; N: flt.psd-hxg.Hd/2lat.apd; O-P: Dn.ml.cvx/crn.lrg; U1, W, X, Y1, AA, AB, AC, AD, AE, AG, AH, AL, AM, AP, AU, AW, BE: 2Ax.brd.br/rd.ax.tp; U2, V, Y2, Z, AO, AQ, AS, AV, AX, AY: 2Ax.brd.br/psd-rtg.ax.tp; AF, AR, BI: 2Ax.brd.br/elg.ax.tp; AI, AK, AT: 2Ax.brd.br/shr.ax.tp; AJ: 2Ax.act.br/ptd.bs/2lat.apd; AZ, BA, BB: 2Ax.brd.br/trg.cvt/ax.tp; BC, BD, BF, BG, BH: 3Ax.brd.br; BK: brd.2Ax/trg.cvt; BL: elg.ml.Tt/tn.flt.crw; BJ: new unnamed morphotype; BM-BQ, BT: cnc.ml.Tt; BR: brd.ml.Tt/tn.flt.crw; BS: cvx.ml.Tt/tn.crw/int.cvt; BU: elg.Br; BV: div.elg.Br; BW: div.elg.Br; BX, BZ: tn.Wg/shr.ax.tp; BY: 2prl.Br/elg.tp; CA-CB: elg.psd-hxg.Hd/2lat.apd; CC-CD: flt.psd-hxg.Hd/2lat.apd. All photomicrographs with the same scale bar = 250 µm. A-C: Ch2b; D-J, L-N, P, R, T: Ch1; K, O, Q, S: Ch4a; U, Y, AL, BD: 36.1; V, BC, BL-BM, BR, BV: 31H; W-X, AP, BE, BK: 38H; Z, AR, AZ, BG, BT, BW: 35M; AA, AM, AQ, BA, BI, BN, BO, CB: 34M; AB, AK, AV, AX, BX: 36.3; AC: 32B; AD: 36.2; AE-AF, BF: 37B; AG, AH, BH: 31B; AI, AO, AS, BP-BQ, BZ, BY, CC: 36.4; AJ: Ch8; AN, AU, BB: 37H; AT, AW: 36.5; AY, BS, CA: 38B; BE: 32/1.2; BJ: 36.6; BU: 40M; CD: 32H. Lower Tithonian: A-C, K, O, Q, S; upper Tithonian: D-J, L-N, P, R, T-CD. Lower Tithonian: A-T; upper Tithonian: U-CD.

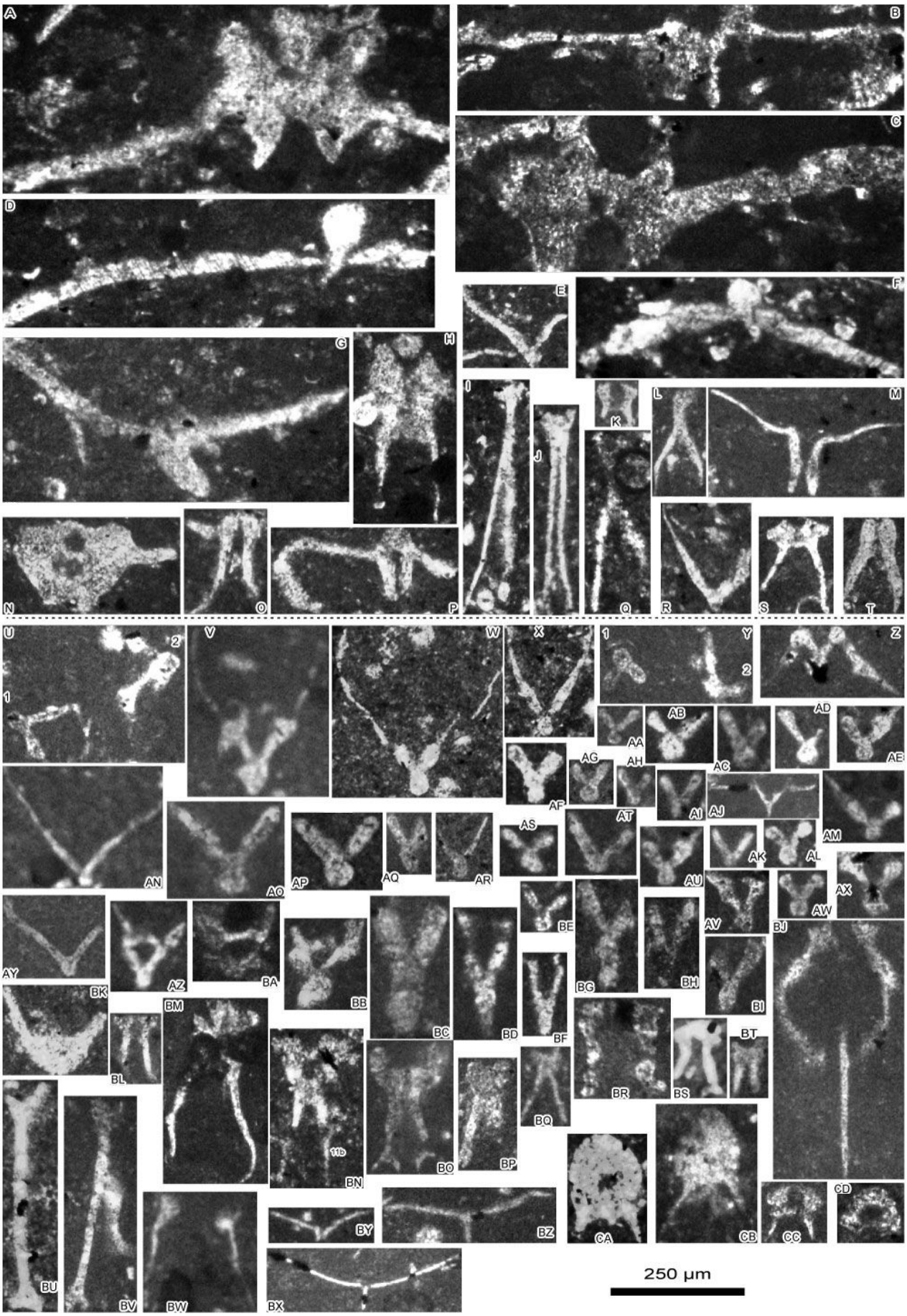
A
B
C
D
E
F
G
H
I
J
K
L
M
N
O
P
Q
R
S
T
U
1
2
V
W
X
Y
Z
AA
AB
AC
AD
AE
AF
AG
AH
AI
AJ
AK
AL
AM
AN
AO
AP
AQ
AR
AS
AT
AU
AV
AW
AX
AY
AZ
BA
BB
BC
BD
BE
BF
BG
BH
BI
BJ
BK
BL
BM
BN
11b
BO
BP
BQ
BR
BS
BT
BU
BV
BW
BX
BY
BZ
CA
CB
CC
CD
250 µm

(subzone A2), and 3) a last one with numerous *Cr. brevis* and *Cr. massutiniana* but also with few *Calpionella elliptalpina* (subzone A3).

5.3.1.1. The **Chitinoidellid-primitive calpionellid Subzone (subzone A0)** spans at least the sampling interval comprised between 36.6 and 36.1. It probably extends downward to the bottom of the breccia Ch7. It is characterized by the assemblage of the last chitinoidellids and the first calpionellids with hyaline tests, mostly primitive forms, with or without small collars. The chitinoidellids comprise representatives of the subfamily Bonetinae, among which *Bonetilla boneti* (DOBEN) and *B. sphaerica* BENZAGGAGH. Calpionellids are represented by primitive forms dominated by *Crassicollaria* aff. *intermedia* DURAND DELGA, small to medium in size (Fig. 14J-K, M-O, R), and also comprise *Calpionella* aff. *alpina* LORENZ, small in size, with ovoid rounded (Fig. 14G) or ovoid elongated (Fig. 14I) loricae, and *Tintinnopsella* aff. *carpathica* (MURGEANU & FILIPESCU) (Fig. 14V-X). We did not observe *T. remanei* BORZA nor *Praetintinnopsella andrusovi* BORZA. Both species are considered by several authors (*e.g.*, REMANE *et al.*, 1986; ÖLVECZKÁ & REHÁKOVÁ, 2022) as subzone indexes of the base of the Crassicollaria Zone, *i.e.*, Remanei Subzone and Praetintinnopsella Subzone respectively.

5.3.1.2. The **Tintinnopsella-Intermedia Subzone (subzone A1)** spans the sampling interval comprised between 35M and 32H. Calpionellids are larger in size than in the previous subzone. The first typical medium-sized *Crassicollaria intermedia* (Fig. 14AE-AF) appears there. It also contains medium-sized *Cr.* aff. *intermedia* (Fig. 14AG), as well as common *Calpionella grandalpina* (Fig. 14Y-AB), small-sized *C. alpina* (Fig. 14AC-AD), and *Crassicollaria* aff. *massutiniana* (Fig. 14AH-AK), and few *Tintinnopsella pseudocarpathica* BENZAGGAGH *et al.* (Fig. 14U) with smaller loricae than those of the genuine *T. carpathica* (MURGEANU & FILIPESCU) from the Berriasian-Valanginian. *Bonetilla boneti* (DOBEN) (Fig. 14F), *B. sphaerica* BENZAGGAGH (Fig. 14E), and primitive calpionellids (Fig. 14L, P-Q, S-T) found in pseudointraclasts of breccia 35 are reworked from the underlying subzone A0.

5.3.1.3. The **Intermedia-Alpina Subzone (subzone A2)** covers the samples 31B to 30H. Typical forms of *Crassicollaria intermedia* DURAND DELGA (Fig. 14AL-AO) are dominating. Their sizes are often larger than those of specimens from the previous subzone. This subzone also commonly contains *Cr. colomi* LORENZ (Fig. 14AQ-AT), *Calpionella grandalpina* NAGY (Fig. 14AY-BA), small-sized *C. alpina* LORENZ (Fig. 14AW-AX), rare *Crassicollaria massutiniana* (COLOM) (Fig. 14AP), *Cr. parvula* REMANE (Fig. 14AU), and *Cr.* aff. *brevis* REMANE (Fig. 14AV).

5.3.1.4. The **Brevis-Massutiniana Subzone (subzone A3)** comprises at least the samples 26/1.0 and 26B. It probably extends downward to the bottom of the breccia 29. Typical forms of *Crassicollaria massutiniana* (COLOM) and *Cr. brevis* REMANE dominate. It also commonly contains small-sized to medium-sized *Calpionella alpina* LORENZ, *C. grandalpina* NAGY, and few *Tintinnopsella pseudocarpathica* BENZAGGAGH *et al.*.

5.3.2. The **Alpina Zone (zone B)**, as originally defined by REMANE (1963), corresponds to an "acmé" interval of the fossil index (*op.cit.*, p. 62: "la prédominance du genre *Calpionella*"). The base of this biozone is not characterized by the first occurrence of *Calpionella alpina* but by the base of its first acme. Some followers of REMANE have focused on identifying "explosions" of *C. alpina*. For instance, WIMBLEDON's summary Figure (WIMBLEDON *et al.*, 2011, Fig. 1) identified not less than "three '*C. alpina*' explosions". However, this "explosion" concept can be misleading as documented by GRANIER *et al.* (2020b, 2023). As a matter of fact, some cryptoturbidites (Fig. 6L, P) are made of well-sorted calpionellid pseudointraclastic micrograinstones, a kind of dynamic accumulation that is not related to any biological bloom (GRANIER *et al.*, 2023).

At Le Chouet, the Alpina Zone starts from breccia 24 (or possibly from turbidite 25 (Fig. 6P), which is locally missing due to the subsequent basal erosion of debris flow 24) upward at least to breccia 10. The physical boundary is aligned with an important change in the calpionellid assemblage that corresponds to the disappearance of the main species of the Crassicollaria Zone, *i.e.*, *Crassicollaria brevis* (Fig. 7E-G), *Cr. colomi*, *Cr. intermedia*, and *Cr. massutiniana* (Fig. 7A-D), which are still found in pseudointraclasts (Fig. 2, red rectangles). *Cr. parvula* is the only representative of the genus *Crassicollaria* to persist in Berriasian times.

▶ **Figure 14:** Chitinoidellid and calpionellid specimens from the upper Tithonian - Boneti Subzone and Crassicollaria Zone (A zone) strata of the Le Chouet section. A-D: Boneti Subzone; G, I-K, M-O, R, V, X: Chitinoidellid - primitive calpionellid Subzone (A0 subzone); E-F, H, L, P-Q, S-T, U, W: material from the Chitinoidellid – primitive calpionellid Subzone (A0 subzone) reworked in the Tintinnopsella-Intermedia Subzone (A1 subzone); Y-AK: Tintinnopsella-Intermedia Subzone (A1 subzone); AL-AP, AU-BA: Intermedia-Alpina Subzone (A2 subzone); AQ-AT: Intermedia-Alpina Subzone (A2 subzone) or ? Brevis-Massutiniana Subzone (? A3 subzone). A: *Bonetilla boneti* (DOBEN); B: *Furrazolaia insueta* (ŘEHÁNEK); C-D*: F. cristobalensis* (FURRAZOLA-BERMÚDEZ); E: *Bonetilla sphaerica* BENZAGGAGH; F: *B. boneti* (DOBEN); G-H: small-sized *Calpionella* aff. *alpina* LORENZ with rounded loricae; I: small-sized *C.* aff. *alpina* LORENZ with ovoid elongated lorica; J-T: *Crassicollaria* aff. *intermedia* DURAND DELGA; U: *Tintinnopsella pseudocarpathica* BENZAGGAGH *et al.*; V-X: *T.* aff. *carpathica* (MURGEANU & FILIPESCU); Y-AB: *Calpionella grandalpina* (…/…)

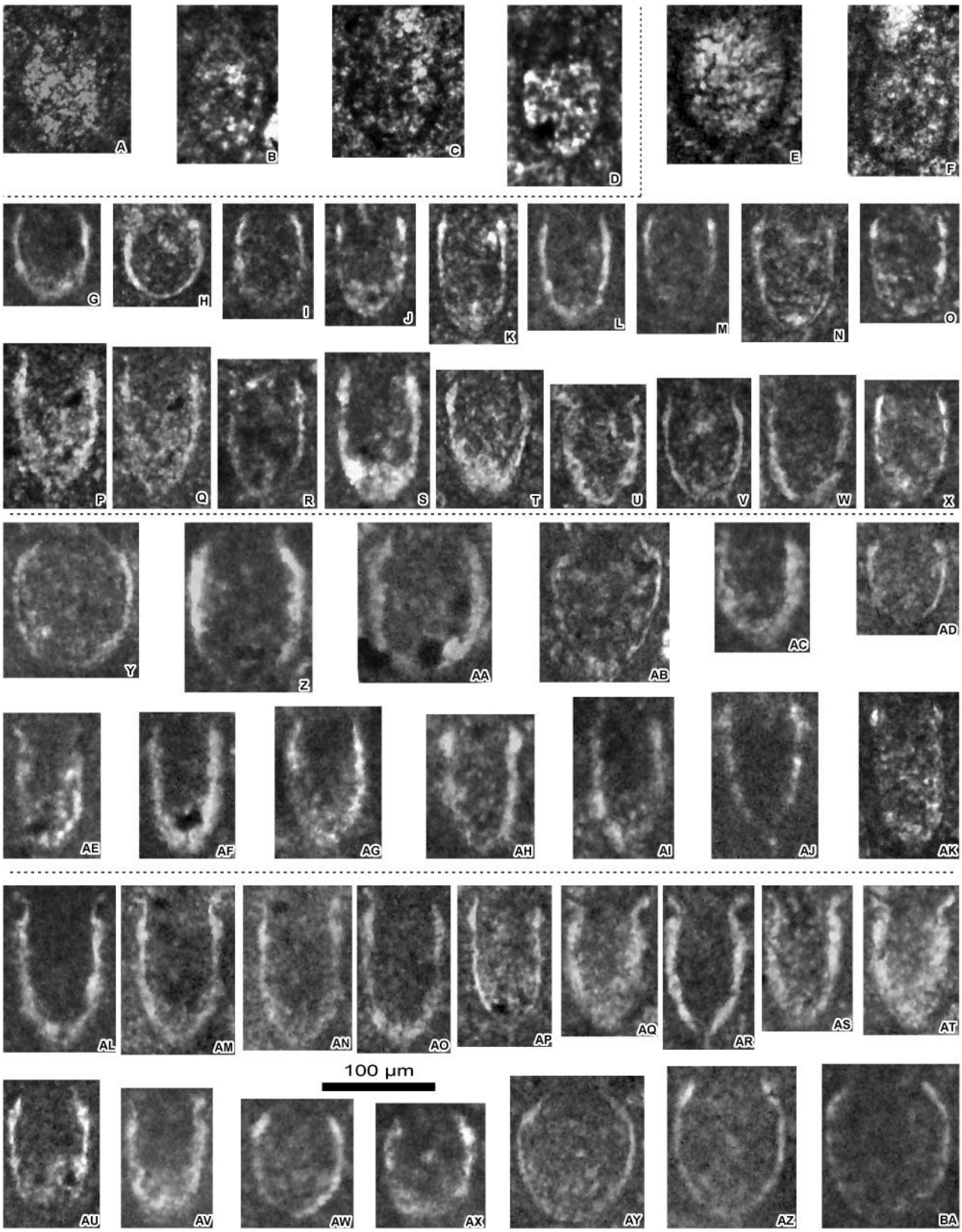

NAGY; AC-AD: small-sized *C. alpina* LORENZ; AE-AG: *Crassicollaria* aff. *intermedia* DURAND DELGA; AH-AK: *Cr.* aff. *massutiniana* (COLOM); AL-AO: *Cr. intermedia* DURAND DELGA; AP: *Cr. massutiniana* (COLOM); AQ-AT: *Cr. colomi* DOBEN; AU: *Cr. parvula*; AV: *Cr.* aff. *brevis*; AW-AX: small-sized *Calpionella alpina* LORENZ; AY-BA: *C. grandalpina* NAGY. All photomicrographs with the same scale bar = 100 µm. A: sample 40M; B-C: sample 37B; D: sample 38B; E-F, H, L, P-Q, S-U, W: sample 35M (reworked specimens from the subzone A0); G, I, N, V: sample 36.6; J-K, R: sample 36.4; M: sample 36.2; O: sample 36.5; X: sample 36.3; Y-AA, AF, AI-AJ: sample 32B; AB, AK: sample 32H; AC-AD, AH: sample 33; AE, AG: sample 34M; AL, AV, BA: sample 31H; AM-AO: sample 31B; AP, AU, AW-AZ: sample 30B; AQ-AT: sample 28 (reworked specimens from the subzone A2).

Only its first subzone, *i.e.*, the Alpina-Parvula Subzone (B1 subzone), has been identified in the Le Chouet section. The abundance of calpionellid loricae contrasts with the low specific diversity of the whole assemblage that consists of –dominating- small-sized *Calpionella alpina* LORENZ (Fig. 7J-L, N-P), -common- *Crassicollaria parvula* (Fig. 7S-T), and -rare- *Tintinnopsella pseudocarpathica* (Fig. 7M).

5.3.2.1. The **Alpina-Parvula Subzone (subzone B1)** is largely dominated by small-sized *Calpionella alpina*, in particular the forms with ovoid rounded loricae (Fig. 7N-P) and ovoid elongated loricae (Fig. 7Q). It also contains common *Crassicollaria parvula* REMANE (Fig. 7R-T) and few *Tintinnopsella pseudocarpathica* BENZAGGAGH *et al.* Within the subzone B1 of the logged section, the breccias commonly contains lithoclasts with specimens of *Calpionella elliptalpina* NAGY (Fig. 7I, U-W), *C. grandalpina* NAGY, *Crassicollaria brevis* and *Cr. intermedia* DURAND DELGA (Fig. 7X), all reworked from the older strata of the Crassicollaria Zone.

6. Discussion

6.1. IMPACT OF SEDIMENTATION AND EROSION RATES ON THE DEFINITION OF BIOZONAL BOUNDARIES

One could argue that a zone or subzone precisely starts with the first occurrence of the proxy (Fig. 15.1). This assumption can be valid when sampling is dense but it is debatable when the sampling frequency is low. For instance, in the illustrated model (Fig. 15.1-2), two samples A (below) and B (above) were picked 1 meter apart. Because we deal with a single lithology, it is assumed that the rate of sedimentation is constant. To simplify the graphical interpretation, the thickness scales (meters) on the left hand side of the columns and the time scales (ka) on their right hand side are congruent. The proxy B is observed in the red zone, not in the blue zone. In this simple model with one lithology (Fig. 15.1-2), the probability that B belongs to the red zone is 100% whereas the probability that A belongs to the red zone is nil. Symmetrically, the probability that A belongs to the blue zone is 100% whereas the probability that B belongs to the blue zone is nil. Depending of its relative sampling distance between A and B, the probability that a sample C picked between A and B belongs to zone B increases when C getting closer to B and decreases when C getting closer to A. On the basis of this approach, the zonal blue/red boundary is drawn as an oblique line, not as a horizontal line (Fig. 15.2).

For example, the base of the Chitinoidella Zone, *i.e.*, the lower/upper Tithonian boundary, at Le Chouet is drawn as an oblique line from the location of sample CH4b up to that of sample 40M, both samples being picked more than 3 meters apart on the log. In alternative approaches, the boundary is commonly ascribed 1) either to the bottom of the B bed when the latter is found between samples B and A, 2) to a median location between samples B and A (that was the option chosen by WIMBLEDON *et al.*, 2020a, Supplement Fig. S1), or 3) to a random location close to sample B (that was the option chosen by WIMBLEDON *et al.*, 2013, p. 444: "The Crassicollaria-Calpionella" (Alpina) "zonal boundary may be placed between 101 and the next sample below", Fig. 4). All these non-probabilistic approaches (either the interpolation or the diagonal boundary) are misleading in the case of Le Chouet (an previously in that of Tré Maroua, GRANIER *et al.*, 2020b, 2023) when a turbidite or debris flow bed occurs between samples B and A.

As discussed above, identifying a zonal boundary can be straightforward when dealing with a single facies because the main concerns will be the sampling frequency and because, after an initial screening, one can always return to the field and densify the sampling around the boundary to better circumscribe it. However, in the case for most of Le Chouet section, two discrete types of facies differ markedly in their net sedimentation rates, which implies adaptation of the simplistic model. The sedimentation rate of the "calcaires blancs" (saccocomid, calpionellid or radiolarian mud- or wackestones) likely represents a relatively constant background basinal sedimentation of a few cm/ka whereas that of the episodic turbidites and debris flows is often higher than several centimeters (or even tens of centimeters) per hour (see GRANIER *et al.*, 2013: Fig. 7.B).

Figure 15.3 illustrates a case with two lithologies where a slice of debris flow occurs within the basinal facies and between the locations of samples A and B. The first column (Fig. 15.3a) corresponds to the lithology versus the thickness; the second column (Fig. 15.3b) corresponds to the lithology versus the time. In a practical case, to convert thickness into time, the thickness of each interval should be divided by the corresponding rate of sedimentation. As previously noted for the single lithology case, the thickness scales (meters) and the time scales (ka) are congruent. The graphical thicknesses remain the same for the "calcaires blancs" but the graphical thickness of the debris flow tends toward zero (Fig. 15.3b), *i.e.*, the graphical representation of a few hours on a ka scale would be a horizontal line. However, the basinal facies above and below the debris flow are not exactly superposed. There is a time gap between them that represents basinal sediment (and possibly turbidites and debris flows) that was removed by erosion at the bottom of the debris flow (Fig. 8).

As stated in GRANIER *et al.* (2023), "There is no relationship" "between the depth of erosion", *i.e.*, the amount of material removed at the erosion surface, "at a location and the amount of material accumulated above the erosion surface at this same location". The duration of such hiatuses is commonly impossible to determine. Following the previously described simplistic approach, the

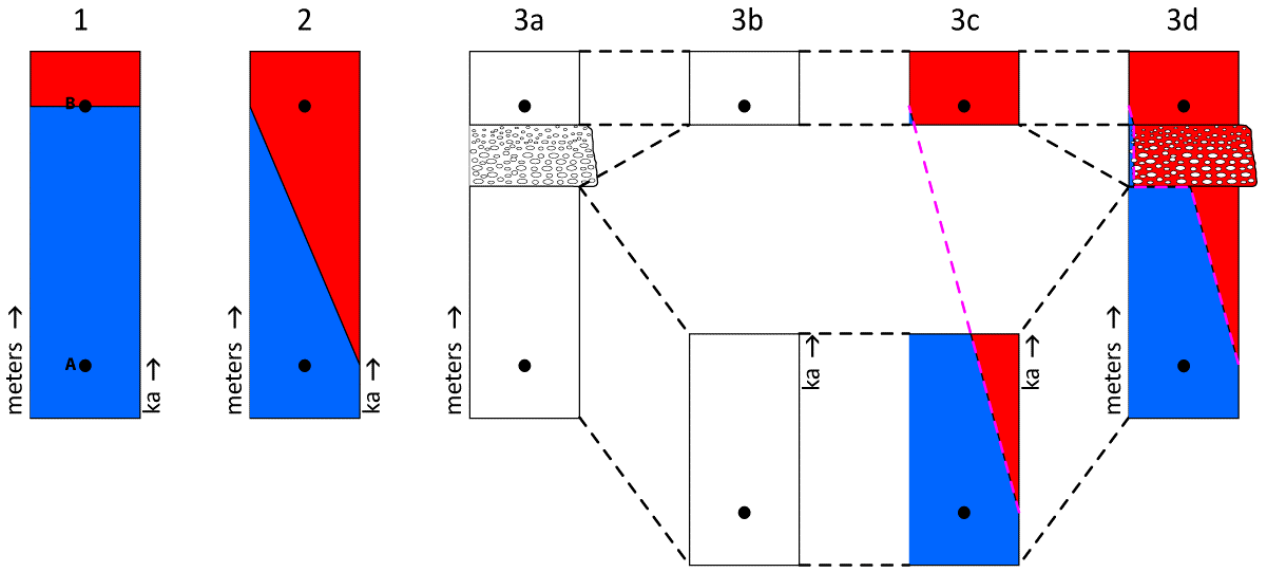

Figure 15: Models for a confident identification of zonal boundaries based on the lithologies and the corresponding sedimentary rates. Sampling rate is not negligible. Erosion rates at the bottom of debris flows and turbitides may vary significantly. See description in the text.

zonal blue/red boundary is drawn as an oblique line (Fig. 15.3c). In order to revert to the original figure (Fig. 15.3a), *i.e.*, to convert again time into thickness, the duration of each interval should be multiplied by the rate of sedimentation for the corresponding lithology. On the new figure, the blue/red boundary is not a straight line anymore (Fig. 15.3d). This last graphical representation makes it clear how, in this case, the debris flow very highly probably belongs to the red zone and that the base of this red zone should be located on the erosional surface at the base of this debris flow. The probability that the red zone extends below the breccia is not nil but quite low. For instance, as documented by GRANIER *et al.* (2020b, 2023) for the Tré Maroua section, the base of the Ferasini Subzone of the Alpina Zone and the base of the M18r magnetozone should be located at the bottom of the uppermost debris flow, *i.e.*, number 69, not at its top as shown in WIMBLEDON *et al.* (2020a: Fig. 4).

Our control on the saccocomid zones or on the Chitinoidella Zone is poor, mainly due to a low sampling frequency in the corresponding interval. For instance, the significant uncertainty on the location of the lower/upper Tithonian boundary is mainly driven by a poor sampling within the interval from sample Ch4b to sample 40M.

In contrast, the bases of the Crassicollaria Zone and subzones and those of the Alpina Zone, hence of its first subzone, are well identified. They systemically correspond to the bottoms of breccia or turbidite layers:

- the base of zone A or subzone A0 matches with the bottom of the thick breccia bed Ch7;
- that of subzone A1 with the bottom of the thick breccia bed set 35 to 33. In sample 35M, *Bonetilla boneti* (DOBEN) (Fig. 14F) and *B. sphaerica* BENZAGGAGH (Fig. 14E) are found reworked in extraclasts derived from the preceding subzone (subzone A0);
- that of subzone A2 with the bottom of the graded breccia bed 31;
- that of subzone A3 is tentatively located at the bottom of turbidite bed 29 of a set comprising the breccia bed 28 sandwiched between the turbidite beds 29 and 27;
- that of zone B or subzone B1 matches with the bottom of the graded breccia bed 24 or locally to the bottom of turbidite bed 25 when the latter was not eroded by the overlying debris flow 24 (Fig. 5H-I).

6.2. DISCREPANCIES IN THE PLACEMENT OF ZONAL BOUNDARIES

Besides the probabilistic or non-probabilistic options and the sampling frequency, the other key factor that generates inherent discrepancies in the location of the zonal boundaries can be differences in the diverse acceptions of species or zones by the various authors. For instance, REHÁKOVÁ (in WIMBLEDON *et al.*, 2013, 2020a) does not refer to *Tintinnopsella pseudocarpathica* BENZAGGAGH *et al.*, 2012, or *Bonetilla sphaerica* BENZAGGAGH, 2021. The various authors do not necessarily use the same subzones (see BENZAGGAGH, 2020, for discussion).

As for the calpionellid biozones, all authors generally share the same view regarding the definitions of the Chitinoidella, Crassicollaria (zone A) and Alpina (zone B) zones. Due to poor sampling and facies that are not favorable to the preservation (or identification) of the chitinelloids, *i.e*, turbidites, the base of the Chitinoidella Zone cannot be accurately identified: It is expected to fall between 9 and 12 m on the log of Figure 2 whereas it would be near 5 m (below our turbidite Ch2) according to REMANE's log (1970) and near 9 m

according to WIMBLEDON *et al.*' (2020a) log. All the authors agree upon the base of the Crassicollaria Zone near 15.5 m (at the bottom of our breccia Ch7) on the log of Figure 2. The main discrepancies occur at the base of the *Calpionella alpina* acme Zone: **1)** REMANE (1970) identifies it at the base of turbidite 22, near 27.7 m; **2)** WIMBLEDON *et al.* near 30 and near 29.5 m in 2013 and in 2020 (2020a) respectively; **3)** we assume that it should be placed at the base of turbidite(s) 24 (or 25), near 26.5 m on the log of Figure 2. It is worth mentioning that the marker for this boundary (*i.e.*, the base of the *Calpionella alpina* acme Zone) was the candidate proxy for the Berriasian GSSP proposed by the past Berriasian Working Group (WIMBLEDON *et al.*, 2013, 2020a). There are also significant discrepancies regarding the subzones of the Crassicollaria Zone. The only agreements are found with 1) the Remanei Subzone of WIMBLEDON *et al.* (2020a) that matches our subzone A0 and 2) the base of the Intermedia Subzone of WIMBLEDON *et al.* (2020a) and that of our subzone A1 because both fall at the base of turbidite 35, near 18 m on the log of Figure 2. The bases of REMANE's (1970) subzones A2 and A3 respectively fall on top of turbidite 33, at 20.5 m, and above turbidite 27, at 25.5 m on the log of Figure 2. The bases of the Intermedia and Colomi subzones of WIMBLEDON *et al.* (2013, 2020a) fall between turbidite 33 and breccia 31, at 22 m for the first one, and below turbidites 24-25, near 26.4 m for the second one. In contrast and as for our previous zones and subzones, the bases of our subzones A2 and A3 correspond to the erosional bases of turbidites or debris flows, *i.e.*, to the base of breccia 31, at 23 m for the first one, and to the base of turbidite 29, at 24.5 m for the second one.

6.3. SIGNIFICANCE OF THE LOCAL EROSION

From the outcrops on the side of the tarred track, the erosional bases of the gravity flows (turbidites and debris flows) at all scales are well exposed (Figs. 4H, 5C, F, H). In Figure 5H, turbidite 25 is partly eroded at the bottom of the debris flow 24. Many extraclasts and other erosional features such as microscopic erosional surfaces are also visible under the binocular microscope (see Fig. 6L here or see GRANIER *et al.*, 2023, Fig. 8E at Tré Maroua).

According to GRANIER *et al.* (2023), "There is inherently no relationship between the thickness of a debris flow or a turbidite layer at a location and the amount of material that was eroded from this same location and that accumulated downdip". Due to the limited temporal resolution of the saccocomid and calpionellid biozones, estimating the depth of erosion is challenging, not to say almost impossible. However, there are a few exceptions. For instance, at Tré Maroua, GRANIER *et al.* (2020b, 2023) reported saccocomid-bearing lithoclasts more than 2 meters and even more than 10 meters above the last saccocomid zone. From the same section, GRANIER *et al.* (2020b, 2023) also documented *Crassicollaria*-bearing lithoclasts (GRANIER *et al.*, 2020b, Pl. 3, figs. B-C) more than 5 meters and even more than 9 meters above the Crassicollaria Zone. At Le Chouet, there are fewer clues. In breccia 24, at 27 m on the log of Figure 2, *i.e.*, at the bottom of the Alpina Zone, *Crassicollaria brevis* REMANE, *Cr. intermedia* DURAND DELGA (Fig. 7X), and *Cr. massutiniana* (COLOM) are found in extraclasts derived from the preceding zone (Crassicollaria Zone). This same *Crassicollaria* assemblage is also observed within the Alpina Zone in breccia 16, at 31.7 m, more than 5 meters above the Crassicollaria Zone.

7. Conclusions

The Le Chouet section spans a Tithonian-lower Berriasian interval. Saccocomid zones 4 to 7 as well as Chitinoidella, Crassicollaria and Alpina zones of the calpionellids have been documented. However, the Dobeni Subzone of the Chitinoidella Zone has not been identified in its lower part and only the first subzone of the Alpina Zone, *i.e.*, the Alpina Subzone, has been documented at its upper part.

Whereas the location of the lower/upper Tithonian boundary remains uncertain (possibly close to Ch4, *i.e.*, near 9 m on the log of Figure 2), the Tithonian/Berriasian boundary defined by calpionellid biostratigraphy coincides with the base(s) of turbidite 25 (or breccia 24 when the previous one has been eroded, *i.e.*, near 26.5 m on the log of Figure 2): Figs. 4A, 5H-I, 6B. That pushes the Tithonian/Berriasian boundary down by almost 1 m relative to REMANE (1970; note that most Crassicollarias found in the interval are here considered to be reworked) and some 4 m relative to WIMBLEDON *et al.* (2013, 2020a).

The foraminifer *Protopeneroplis ultragranulata* (GORBATCHIK) is the index of the *P. ultragranulata* Subzone of the *Anchispirocyclina lusitanica* Zone (Tithonian-lower Berriasian). This microfossil was supposed to first occur in the late Tithonian (BUCUR, 1997) and the eponymic subzone to span the upper Tithonian-lower Berriasian interval (GRANIER, 2019; GRANIER *et al.*, 2020a). However, its find in upper lower Tithonian strata (Fig. 12AC, sample Ch2b) extends its subzone downwards. GRANIER (2019) stated that "it is impossible to distinguish the (upper) Tithonian from the lower Berriasian" in the shallow-water facies of the Tethys realm. This wider range for the index of the subzone drives the nail deeper into the coffin. This argument, together with the lack of biological crisis and the instability of the boundary definition and location, supports the assessment that the default Tithonian/Berriasian boundary (*i.e.*, base of the *Calpionella alpina* "acme" Zone) is a poor system boundary. In contrast, as stated by ÉNAY (2020), "the base Valanginian, which corresponds to biotic crises affecting the ammonites and other groups, is by far the better alternative" for "the Jurassic/Cretaceous system boundary".

The frequency of gravity-flow (debris flows and turbidites, including cryptoturbidites) led us to reassess the calpionellid stratigraphy with the eyes of sedimentologists. All bases of calpionellid zones and subzones (except those of the Chitinoidella Zone and its Boneti Subzone) are located at basal erosional surfaces of turbidites or debris flows. Accordingly, as in the Tré Maroua section (GRANIER *et al.*, 2020b, 2023), all these zonal boundaries are probably hiatal here too. As already explained in GRANIER *et al.* (2023), not only these two localities but even "a wider region in the Vocontian Trough", which is affected by "paleotectonic instability", should enevitably fail to provide any suitable Berriasian GSSP candidate "in contradiction with the expectations of the 'Colloque sur la limite Jurassique/Crétacé' held in Lyon in 1973 (FLANDRIN *et al.*, 1975)". It is worth mentioning that corresponding time gaps at erosional surfaces, even if short, artificially emphasise the contrasts between the successive calpionellid assemblages.

The depth of erosion at the bottom of any gravity-flow bed can hardly be estimated in any single site. However, because pebbles and cobbles sourced from the Crassicollaria Zone are reported at Le Chouet some 5 m above the local top of this zone, it is assumed that the depth of erosion could have reached more than 5 m in some updip locations. On the basis of data from the Tré Maroua site (GRANIER *et al.*, 2020b, 2023), it can even be estimated that updip depth of erosion could have locally reached 10 m or more. Considering published regional data (COURJAULT, 2011; COURJAULT *et al.*, 2011; FERRY *et al.*, 2015; FERRY, 2017), such deep erosional features did not result from a single episode but probably from multiple, successive episodes digging each time deeper into the preexisting sedimentary substratum.

Acknowledgements

Field work was made possible thanks to a grant from the Foundation "Carnets de Géologie". Part of this work was presented on the occasion of JK2018 - International Meeting around the Jurassic/Cretaceous Boundary held in Genève (Switzerland) from December 5th to 7th, 2018 (FERRY & GRANIER, 2018), and of the 11th International Cretaceous Symposium held in Warsaw (Poland) from August 22th to 26th, 2022 (GRANIER *et al.*, 2022). It is a contribution to Project no. 46908YB of the PHC ("Partenariats Hubert CURIEN") Polonium 2022. The manuscript was originally submitted to *Geologica Carpathica* and later withdrawn due to requests to remove or modify some key figures. However, the authors are grateful to the two reviewers and the editor for their comments and suggestions that helped improve the original manuscript. Special thanks are also due to Phil SALVADOR who kindly checked the final version of our English text.

Bibliographic references

BENZAGGAGH M. (2020).- Discussion on the calpionellids biozones and proposal of a homogeneous calpionellid zonation for the Tethyan Realm.- *Cretaceous Research*, vol. 113, article 104184, 24 p.

BENZAGGAGH M. (2021).- Systematic revision and evolution of the Tithonian family Chitinoidellidae TREJO, 1975.- *Carnets Geol.*, Madrid, vol. 21, no. 2, p. 27-53.

BENZAGGAGH M., CECCA F., SCHNYDER J., SEYED-EMAMI K. & MAJIDIFARD M.R. (2012).- Calpionelles et microfaunes pélagiques du Jurassique supérieur-Crétacé inférieur dans les formations Shal et Kolur (Montagnes du Talesh, chaîne de l'Elbourz, Nord-Ouest Iran). Répartition stratigraphique, espèces nouvelles, révision systématique et comparaisons régionales.- *Annales de Paléontologie*, Paris, vol. 98, no. 4, p. 253-301.

BENZAGGAGH M., HOMBERG C., SCHNYDER J. & BEN ADESSELAM-MAHDAOUI S. (2015).- Description et biozonation des sections de crinoïdes saccocomidés du Jurassique supérieur (Oxfordien-Tithonien) du domaine téthysien occidental.- *Annales de Paléontologie*, Paris, vol. 101, p. 95-117.

BUCUR I.I. (1997).- Representatives of the genus *Protopeneroplis* (foraminifera) in the Jurassic and Lower Cretaceous deposits from Romania. Comparisons with other regions of the Tethyan realm.- *Acta Palaeontologica Romaniae*, Cluj-Napoca, vol. 1, p. 65-71 (Pls. 6.I-III).

CECCA F., ÉNAY R. & LE HÉGARAT G. (1989).- L'Ardescien (Tithonique supérieur) de la région stratotypique : Séries de référence et faunes (ammonites, calpionelles) de la bordure ardéchoise.- *Documents des Laboratoires de Géologie de Lyon*, Villeurbanne, vol. 107, 115 p.

COURJAULT T. (2011).- Brèches gravitaires sous-marines du Tithonien subalpin (S-E France).- PhD thesis, Université de Strasbourg, 339 p.

COURJAULT T., GROSHENY D., FERRY S. & SAUSSE J. (2011).- Detailed anatomy of a deep-water carbonate breccia lobe (Upper Jurassic, French subalpine basin).- *Sedimentary Geology*, vol. 238, no. 1-2, p. 156-171.

ÉNAY R. (2020).- The Jurassic/Cretaceous System Boundary is at an impasse. Why not go back to OPPEL's 1865 original and historic definition of the Tithonian?- *Cretaceous Research*, vol. 106, article 104241, 20 p. DOI: 10.1016/j.cretres.2019.104241

FERRY S. (2017).- Summary on Mesozoic carbonate deposits of the Vocontian Trough (Subalpine Chains, SE France). *In*: GRANIER B. (ed.): Some key Lower Cretaceous sites in Drôme (SE France).- Association Carnets de Géologie, Madrid, CG2017_B01, p. 9-42. DOI: 10.4267/2042/62543

FERRY S. & GRANIER B. (2018).- 12. Looking for the Jurassic-Cretaceous system boundary in the Vocontian Trough (S-E France): Sedimentological problems. *In*: GRANIER B. (ed.), JK2018 - International Meeting around the Jurassic-Cretaceous Boundary.- Association Carnets de Géologie, Madrid, CG2019_B01, p. 24 (abstract). DOI: 10.4267/2042/69811

FERRY S., GROSHENY D., BACKERT N. & ATROPS F. (2015).- The base-of-slope carbonate breccia system of Céüse (Tithonian, S-E France): Occurrence of progradational stratification in the head plug of coarse granular flow deposits.- *Sedimentary Geology*, vol. 317, p. 71-86.

FLANDRIN J. (1970).- Luc-en-Diois.- *Carte géologique détaillée de la France au 1/50 000*, Orléans, Feuille 0868, Notice XXXII-38, 19 p., 1 map.

FLANDRIN J., SCHAER J.-P., ÉNAY R., REMANE J., RIO M., KUBLER B., LE HÉGARAT G., MOUTERDE R. & THIEULOY J.-P. (1975).- Colloque sur la limite Jurassique/Crétacé, Lyon-Neuchâtel, 1973. *Mémoires du Bureau de Recherches Géologiques et Minières*, Orléans, vol. 86, 393 p.

GRANIER B. (2019).- Dual biozonation scheme (benthic foraminifera and "calcareous" green algae) over the Jurassic-Cretaceous transition. Another plea to revert the system boundary to its historical ORBIGNY's and OPPEL's definition. *In*: GRANIER B. (ed.), VSI: The transition of the Jurassic to the Cretaceous: An early XXIth century holistic approach.- *Cretaceous Research*, vol. 93, p. 245-274.

GRANIER B., BENZAGGAGH M. & FERRY S. (2023).- Revised holostratigraphy of the Tithonian-Berriasian transition at Tré Maroua (Le Saix, Hautes-Alpes, SE France): Study of a rejected Berriasian GSSP candidate.- *Volumina Jurassica*, Varsaw, vol. XXI, p. 1-18.

GRANIER B., CLAVEL B., MOULLADE M., BUSNARDO R., CHAROLLAIS J., TRONCHETTI G. & DESJACQUES P. (2013).- L'Estellon (Baronnies, France), a "Rosetta Stone" for the Urgonian biostratigraphy.- *Carnets Geol.*, Madrid, vol. 13, no. A04, CG2013_A04, p. 163-207. DOI: 10.4267/2042/51213

GRANIER B., ÉNAY R. & CHAROLLAIS J. (2020a).- News and Reviews - Discussion of the paper by WIMBLEDON *et al.*, 2020b, entitled "The proposal of a GSSP for the Berriasian Stage (Cretaceous System): Part 1" [*Volumina Jurassica*, XVIII (1)].- *Volumina Jurassica*, Varsaw, vol. XVIII, no. 2, p. 237-250.

GRANIER B., FERRY S. & BENZAGGAGH M. (2020b).- A critical look at Tré Maroua (Le Saix, Hautes-Alpes, France), the Berriasian GSSP candidate section.- *Carnets Geol.*, Madrid, vol. 20, no. 1, p. 1-17. DOI: 10.4267/2042/70714

GRANIER B., FERRY S. & BENZAGGAGH M. (2022).- Calpionellid biostratigraphy judged by the yardstick of sedimentology. *In*: 11th International Cretaceous Symposium.- Abstract Volume, Talk_S10, p. 176-177 (abstract).

JAIN S., MULUGETA M., BENZAGGAGH M., SALAMON M.A. & SCHMEROLD R. (2021).- Discovery of chitinoidellids and calpionellids from the Blue Nile Basin and the Jurassic-Cretaceous boundary in Ethiopia.- *Cretaceous Research*, vol. 132, article 105112, 17 p.

KIETZMANN D.A. (2017).- Chitinoidellids from the Early Tithonian-Early Valanginian Vaca Muerta Formation in the Northern Neuquén Basin, Argentina.- *Journal of South American Earth Sciences*, vol. 76, p. 152-164.

KIETZMANN D.A., IGLESIA LLANOS M.P., GONZÁLEZ TOMASSINI F., LANUSSE NOGUERA I., VALLEJO D. & HERNÁN REIJENSTEIN R. (2021).- Upper Jurassic-Lower Cretaceous calpionellid zones in the Neuquén Basin (Southern Andes, Argentina): Correlation with ammonite zones and biostratigraphic synthesis.- *Cretaceous Research*, vol. 127, article 104950, 28 p.

LE HÉGARAT G. (1973).- Le Berriasien du Sud-Est de la France.- Thèse Docteur ès Sciences naturelles 149 (1971), Université Claude BERNARD - Lyon; *Documents du Laboratoire de Géologie de la Faculté de Lyon*, Villeurbanne, vol. 43, 576 p.

ÖLVECZKÁ D. & REHÁKOVÁ D. (2022).- Upper Tithonian Crassicollaria Zone: New data on the calpionellid distribution and subzonal division of the Pieniny Klippen Belt in Western Carpathians.- *Acta Geologica Slovaca*, Bratislava, vol. 14, no. 1, p. 37-56.

POSTMA G., NEMEC W. & KLEINSPEHN K.L. (1988).- Large floating clasts in turbidites: A mechanism for their emplacement.- *Sedimentary Geology*, vol. 58, no. 1, p. 47-61.

REMANE J. (1963).- Les calpionelles dans les couches de passage Jurassique-Crétacé de la fosse vocontienne.- *Travaux du Laboratoire de Géologie de la Faculté des Sciences de Grenoble*, vol. 39, p. 25-82.

REMANE J. (1970).- Die Entstehung der resedimentären Breccien im Obertithon der subalpinen Ketten Frankreichs.- Dissertation (1969), Göttingen; *Eclogae geologicae Helvetiae*, Basel, vol. 63, no. 3, p. 685-740.

REMANE J., BAKALOVA-IVANOVA D., BORZA K., KNAUER J., NAGY I., POP G. & TARDI-FILÁCZ E. (1986).- Agreement on the subdivision of the standard calpionellid zones defined at the Iind planktonic conference, Roma 1970.- *Acta Geologica Hungarica*, Budapest, vol. 29, no. 1-2, p. 5-14.

SCHLAGINTWEIT F. & GAWLICK H.-J. (2011).- *Perturbatacrusta leini* n. gen., n. sp. a new microencruster *incertae sedis* (? sponge) from Late Jurassic to earliest Cretaceous platform margin carbonates of the Northern Calcareous Alps of Austria.- *Facies*, Erlangen, vol. 57, p. 123-135.

WIMBLEDON W.A.P., CASELLATO C.E., REHÁKOVÁ D., BULOT L.G., ERBA E., GARDIN S., VERREUSSEL R.M.C.H., MUNSTERMAN D.K. & HUNT C. (2011).- Fixing a basal Berriasian and Jurassic-Cretaceous (J-K) boundary - Perhaps there is some light at the end of the tunnel?- *Rivista Italiana*

di Paleontologia e Stratigrafia, Milano, vol. 117, no. 2, p. 295-307.

WIMBLEDON W.A.P., REHÁKOVÁ D., PSZCZÓŁKOWSKI A., CASELLATO C.E., HALÁSOVÁ E., FRAU C., BULOT L.G., GRABOWSKI J., SOBIEŃ K., PRUNER P., SCHNABL P. & ČÍŽKOVÁ K. (2013).- An account of the bio- and magnetostratigraphy of the Upper Tithonian-Lower Berriasian interval at Le Chouet, Drôme (SE France).- *Geologica Carpathica*, Bratislava, vol. 64, no. 6, p. 437-460.

WIMBLEDON W.A.P, REHÁKOVÁ D., SVOBODOVÁ A., SCHNABL P., PRUNER P., ELBRA T., ŠIFNEROVÁ K., KDÝR Š., FRAU C., SCHNYDER J. & GALBRUN B. (2020a).- Fixing a J/K boundary: A comparative account of key Tithonian-Berriasian profiles in the departments of Drôme and Hautes-Alpes, France.- *Geologica Carpathica*, Bratislava, vol. 71, no. 1, p. 24-46.

WIMBLEDON W.A.P, REHÁKOVÁ D., SVOBODOVÁ A., ELBRA T., SCHNABL P., PRUNER P., ŠIFNEROVÁ K., KDÝR Š., DZYUBA O., SCHNYDER J., GALBRUN B., KOŠŤÁK M., VAŇKOVÁ L., COPESTAKE P., HUNT C.O., RICCARDI A., POULTON T.P., BULOT L.G., FRAU C. & DE LENA L. (2020b).- The proposal of a GSSP for the Berriasian Stage (Cretaceous System): Part 1.- *Volumina Jurassica*, Varsaw, vol. XVIII, no. 1, p. 53-106.